

VIII. *Stability of a Viscous Liquid contained between Two Rotating Cylinders.*

By G. I. TAYLOR, F.R.S.

Received March 21,—Read April 6, 1922.

[PLATES 4 AND 5.]

PART I.—THEORETICAL.*

Introduction.

IN recent years much information has been accumulated about the flow of fluids past solid boundaries. All experiments so far carried out seem to indicate that in all cases† steady motion is possible if the motion be sufficiently slow, but that if the velocity of the fluid exceeds a certain limit, depending on the viscosity of the fluid and the configuration of the boundaries, the steady motion breaks down and eddying flow sets in.

A great many attempts have been made to discover some mathematical representation of fluid instability, but so far they have been unsuccessful in every case. The case, for instance, in which the fluid is contained between two infinite parallel planes which move with a uniform relative velocity has been discussed by KELVIN, RAYLEIGH, SOMMERFELD, ORR, MISES, HOPF, and others. Each of them came to the conclusion that the fundamental small disturbances of this system are stable. Though it is necessarily impossible to carry out experiments with infinite planes, it is generally believed that the motion in this case would be turbulent, provided the relative velocity of the two planes were sufficiently great.

Various suggestions have been made to account for the apparent divergence between theory and experiment. Among the most recent is that of HOPF, who points out that the flow would be unstable if the two infinite planes were flexible, so that the pressure could remain constant along them. There seems little to recommend this theory as an explanation of the observed turbulent motion of fluids, for there is no experimental evidence that instability is in any way connected with want of rigidity in the solid boundaries of the fluid. The more generally accepted view that infinitely small

* A Summary of both parts of this paper will be found at 'Roy. Soc. Proc.,' A, vol. 102, p. 541.

† All cases where there is relative motion between the fluid and the boundaries, thus excluding the case of steady rotation of a liquid in a rotating vessel.

disturbances are stable, but that disturbances of finite size tend to increase, seems to be more in accordance with the experimental evidence, for it has been shown by OSBORNE REYNOLDS that the velocity at which water flowing through a pipe becomes turbulent depends to a very large extent on the amount of initial disturbance in the reservoir from which the water originally came.

On the other hand it has not yet been shown that disturbances of small but finite size do increase in such a manner as to give rise to the large disturbances observed in cases of turbulent motion.

So far all attempts to calculate the speed at which any type of flow would become unstable have failed. The most promising perhaps was that of OSBORNE REYNOLDS who assumed an arbitrary disturbance in the flow and determined whether it would tend to increase or decrease initially. As applied by REYNOLDS himself this method does not lead to any definite result. It does not determine an upper limit to the speed of flow which must be stable because some other type of disturbance might exist which would increase initially at a lower speed of the fluid. Neither does it determine a lower limit to the speeds at which the flow must be unstable, because the assumed disturbance which initially increases might decrease indefinitely at some later stage of the motion. It has been shown in fact that certain types of initial disturbance exist for which this actually is the case.*

The method of OSBORNE REYNOLDS has been modified by ORR, who has determined in two cases† the highest speed of flow at which all small disturbances initially decrease. At this speed evidently any initial small disturbance will decrease indefinitely.

ORR's method gives the only definite result which has yet been obtained in the subject. The result, however, is merely a negative one, in that it affords no indication as to whether flow at high speeds would be unstable. ORR's result, for instance, in the case of flow through a pipe of circular cross-section is that when the mean speed, W , of the fluid is less than the value given by $W = 180 \nu/D$, D being the diameter of the pipe and ν the kinematic viscosity, the motion will be stable. The value of W so obtained is less than 1/70th of the highest speed at which the flow has been observed to be stable under suitable experimental conditions. ORR's method therefore is of very little assistance in understanding the observed instability of fluid flow.

Indeed, ORR remarks in the introduction to his paper: "It would seem improbable that any sharp criterion for stability of fluid motion will ever be arrived at mathematically."

Scope of the Present Work.

It seems doubtful whether we can expect to understand fully the instability of fluid flow without obtaining a mathematical representation of the motion of a fluid in some particular case in which instability can actually be observed, so that a detailed comparison can be made between the results of analysis and those of experiment. In

* ORR, "Stability or Instability of Motions of a Viscous Fluid," 'Proc. Roy. Irish Acad,' 1907, p. 90.

† *Loc. cit.*, p. 134.

the following pages a special type of fluid instability is discussed and experiments are described in which the results of analysis are subjected to numerical verification.

The attention of mathematicians has been concentrated chiefly on the problem of the stability of motion of a liquid contained between two parallel planes which move relatively to one another with a uniform velocity. This problem has been chosen because it seemed probable that the mathematical analysis might prove comparatively simple; but even when the discussion is limited to two-dimensional motion it has actually proved very complicated and difficult. On the other hand it would be extremely difficult to verify experimentally any conclusions which might be arrived at in this case, because of the difficulty of designing apparatus in which the required boundary conditions are approximately satisfied.

It is very much easier to design apparatus for studying the flow of fluid under pressure through a tube, or the flow between two concentric rotating cylinders. The experiments of REYNOLDS and others suggest that in the case of flow through a circular tube, infinitely small disturbances are stable, while larger disturbances increase, provided the speed of flow is greater than a certain amount. The study of the fluid stability when the disturbances are not considered as infinitely small is extremely difficult. It seems more promising therefore to examine the stability of liquid contained between concentric rotating cylinders. If instability is found for infinitesimal disturbances in this case it will be possible to examine the matter experimentally.

Stability of Viscous Liquid contained between Two Concentric Rotating Cylinders.

Previous work on the subject.—The stability of an *inviscid* fluid moving in concentric layers has been studied by the late Lord RAYLEIGH. Perfect slipping was assumed to take place at the two bounding cylinders. If the motion is confined to two dimensions his conclusion is that the motion is stable if the liquid is initially flowing steadily with the same distribution of velocity which a viscous liquid would have if confined between two concentric rotating cylinders. All two-dimensional motions of an incompressible fluid, which do not involve change in area of internal boundaries are unaffected by a rotation of the whole system, so that this result merely depends on the existence of a *relative* angular velocity of the two cylinders.

In the case when the disturbances are assumed to be symmetrical about the axis, Lord RAYLEIGH* developed an analogy with the stability of a fluid of variable density under the action of gravity. In this analogy the varying centrifugal force of the different layers of fluid plays the part of gravity and the resulting condition for stability is that the square of the circulation must increase continuously in passing from the inner to the outer cylinder, just as the density of a fluid under gravity must decrease continuously with height in order that it may be in stable equilibrium. This condition leads to the conclusion that if the initial flow of the *inviscid* fluid is the same as that of a viscous fluid in steady motion, this flow will be unstable if the two cylinders are rotating

* "On the Dynamics of Revolving Fluids," 'Roy. Soc. Proc.,' A, 1916, pp. 148-154.

in opposite directions. If they rotate in the same direction then the motion is stable or unstable according as $\Omega_2 R_2^2$ is greater or less than $\Omega_1 R_1^2$. Ω_1 and Ω_2 are the angular velocities of the inner and outer cylinders respectively, while R_1 and R_2 are their radii.

The investigations of KELVIN, ORR, SOMMERFELD, MISES and HOPF on the stability of a viscous fluid shearing between two planes have not been extended to the cylindrical case, but recently W. J. HARRISON* has extended ORR's method to find the maximum relative speed which the two cylinders can possess in order that the energy of *all* possible types of initial disturbance may initially decrease. In this work HARRISON assumes that the motion is two-dimensional. His value for REYNOLD'S criterion therefore contains only the *relative* speeds of the two cylinders. It is unaltered if the whole system is rotated uniformly at any speed. His criterion is therefore the same whether the inner cylinder is fixed and the outer one rotated or *vice versa*.

The question has been investigated experimentally by COUETTE† and MALLOCK.‡

In the experiments of COUETTE the inner cylinder was fixed while the outer one rotated. It was found that the moment of the drag which the fluid exerted on the inner cylinder was proportional to the velocity of the outer cylinder, provided that velocity was less than a certain value. As the speed of the outer cylinder increased above this value the drag increased at a greater rate than the velocity. The change was attributed to a change from steady to turbulent motion. RAYLEIGH'S theory of stability of an inviscid fluid for symmetrical disturbances makes the case when the inner cylinder is fixed stable at all speeds.

MALLOCK'S experiments yielded the same result as COUETTE'S, but in this case the value of REYNOLD'S criterion was higher than that obtained by COUETTE.§

MALLOCK extended his experiments to cover the case in which the inner cylinder rotated and the outer one was at rest. In this case he found instability at all speeds of the inner cylinder. This result is in accordance with Lord RAYLEIGH'S theoretical prediction for the case of an inviscid fluid, but on the other hand it seems certain, in fact Lord RAYLEIGH|| has proved, that at very low speeds all steady motions of a viscous fluid must be stable.

In spite of these differences between theory and experiment there is one point in which RAYLEIGH'S "inviscid fluid" theory is in agreement with MALLOCK'S experiments, namely, the large difference in regard to stability between the cases when the inner and when the outer cylinder is fixed. This shows clearly that in the case when the outer cylinder is fixed at any rate, the disturbance is not two-dimensional in character. Whether it is actually of a symmetrical type as contemplated by RAYLEIGH, or whether it is of some other three-dimensional form, remains to be seen.

* W. J. HARRISON, 'Proc. Camb. Phil. Soc.,' 1921, p. 455.

† 'Ann. de Chim. et de Phys.,' 6^{me} sér., vol. 21, 1890.

‡ 'Phil. Trans.,' A, 1896, p. 41.

§ See ORR, 'Proc. Roy. Irish Acad.,' vol. 27, 1907-9, p. 78.

|| RAYLEIGH, 'Phil. Mag.,' vol. 26, pp. 776-786, 1913.

The most striking feature of Lord RAYLEIGH'S theory for inviscid fluids is the criterion for stability when both cylinders are rotating in the same direction, namely, $\Omega_2 R_2^2 > \Omega_1 R_1^2$. Owing to the construction of their apparatus no information as to the correctness of this criterion of stability is obtainable from the experiments of either MALLOCK or COUETTE.

Author's Preliminary Experiments.

For this reason I decided to construct a rough apparatus in which the two cylinders could be rotated separately. The experiments performed with this apparatus are described in a preliminary paper.* The results appeared to show that the criterion $\Omega_2 R_2^2 > \Omega_1 R_1^2$ is approximately satisfied in a viscous fluid, but that RAYLEIGH'S result is not true for the case when the two cylinders are rotating in opposite directions. The experiments also indicated that the type of disturbance which is formed when instability occurs is symmetrical. These results encouraged me to embark on the complicated problem of trying to calculate the possible symmetrical disturbances of a viscous liquid contained between two rotating cylinders, and at the same time I started to construct an apparatus for observing as accurately as possible the conditions under which instability arises.

The complexity of the mathematical problem arises from the fact that it is necessary to obtain a three-dimensional solution of the equations of motion in which all three components of velocity vanish at both the cylindrical boundaries.

Stability for Symmetrical Disturbances.

Before proceeding to the details of the solution of the problem it may be helpful to readers to give a list of the symbols employed. In Table I. the number of the page on which each symbol is defined is given.

TABLE I.—List of Symbols used, with number of page on which they first appear or are first defined.

(V, Ω_1 , Ω_2 , R_1 , R_2 , A, B, r , μ), p. 294 ;	(z , t , u , v , w), p. 294 ;
(p , ρ , ν , ∇_1^2 , u_1 , v_1 , w_1 , λ , σ), p. 295 ;	($J_1(\kappa_s r)$, $W_1(\kappa_s r)$, C_1 , C_2), p. 296 ;
($B_0(\kappa_s r)$, $B_1(\kappa_s r)$, κ_1 , κ_2 , κ_3 , ...), p. 296 ;	(H_s), p. 297 ;
(a_m , C_3 , C_4 , λ' , b_m , i), p. 298 ;	(C_5 , C_6 , C_7 , c_m), p. 299 ;
(C'_5 , C'_6 , C'_7 , d_m), p. 300 ;	(c_m), p. 301 ;
(L'_m , Δ_1), p. 302 ;	(d), p. 304 ;
(x , $C'_1 C'_2$, ϵ'), p. 305 ;	(y , κ), p. 306 ;
(α , β , γ , η), p. 307 ;	(θ , L_m), p. 308 ;
(Δ_2), p. 308 ;	(P), p. 309 ;
(P'), p. 310 ;	(Δ_3 , ϵ), p. 314 ;
(f_1), p. 315 ;	(f_2 , $\delta_1 P$, P_1), p. 316 ;
(Δ_{11} , Δ_{22} , ... Δ_{88}), p. 319 ;	(ψ), p. 321 ;
(M_1 , M_2 , ... M_8), p. 324.	

* TAYLOR, 'Camb. Phil. Soc. Proc.,' 1921.

Steady Motion.

Let V be the velocity at any point of an incompressible viscous fluid in steady motion between two infinitely long concentric rotating cylinders of radii R_1 and R_2 ($R_2 > R_1$). If r is the distance of a point from the axis then it is known that

$$V = Ar + B/r, \dots \dots \dots (1.0)$$

when A and B are constants which are connected with the angular velocities Ω_1 and Ω_2 of the two cylinders by the relations

$$\left. \begin{aligned} \Omega_1 &= A + B/R_1^2, \\ \Omega_2 &= A + B/R_2^2. \end{aligned} \right\} \dots \dots \dots (1.1)$$

Solving these equations A and B can be expressed in terms of R_1 , R_2 , Ω_1 and Ω_2 and

$$A = \frac{R_1^2 \Omega_1 - R_2^2 \Omega_2}{R_1^2 - R_2^2} = \frac{\Omega_1 (1 - R_2^2 \mu / R_1^2)}{1 - R_2^2 / R_1^2}, \dots \dots \dots (1.2)$$

$$B = \frac{R_1^2 \Omega_1 (1 - \mu)}{1 - R_1^2 / R_2^2}, \dots \dots \dots (1.3)$$

where $\mu = \Omega_2 / \Omega_1$.

Specification of Symmetrical Disturbance.

Let u , $V+v$, w , be the components of velocity in a disturbed motion, u is the component in an axial plane and perpendicular to the axis, $V+v$ is the component perpendicular to the meridian plane and to the axis—that is, in the direction of the undisturbed motion— w is the component parallel to the axis. The scheme is represented in fig. 1.

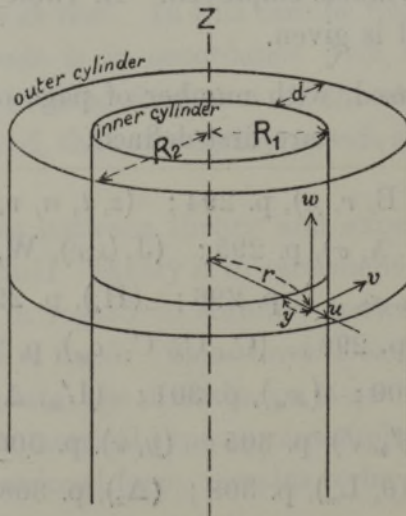


Fig. 1. Scheme of co-ordinates.

We shall assume that u , v and w are small compared with V , and that the disturbance is symmetrical, so that they are functions of r , z and t only; z is the co-ordinate parallel to the axis and t is the time.

Equations of Motion.

Neglecting terms containing products or squares of u , v , w , the equations of disturbed motion may be written

$$\frac{1}{\rho} \frac{\partial p}{\partial r} - \frac{V^2}{r} = -\frac{\partial u}{\partial t} + 2\left(A + \frac{B}{r^2}\right)v + \nu\left(\nabla_1^2 u + \frac{\partial^2 u}{\partial z^2} - \frac{u}{r^2}\right), \dots \dots \dots (2.0)$$

$$0 = -\frac{\partial v}{\partial t} - 2Au + \nu\left(\nabla_1^2 v + \frac{\partial^2 v}{\partial z^2} - \frac{v}{r^2}\right), \dots \dots \dots (2.1)$$

$$\frac{1}{\rho} \frac{\partial p}{\partial z} = -\frac{\partial w}{\partial t} + \nu\left(\nabla_1^2 w + \frac{\partial^2 w}{\partial z^2}\right), \dots \dots \dots (2.2)$$

where p represents pressure, ρ density, ν is kinematic viscosity, and ∇_1^2 represents the operator $\frac{\partial^2}{\partial r^2} + \frac{1}{r} \frac{\partial}{\partial r}$.

The equation of continuity is

$$\frac{\partial u}{\partial r} + \frac{u}{r} + \frac{\partial w}{\partial z} = 0. \dots \dots \dots (2.3)$$

The six boundary conditions which must be satisfied are

$$u = v = w = 0 \text{ at } r = R_1 \text{ and } r = R_2. \dots \dots \dots (2.4)$$

Assume as a solution

$$\left. \begin{aligned} u &= u_1 \cos \lambda z e^{\sigma t}, \\ v &= v_1 \cos \lambda z e^{\sigma t}, \\ w &= w_1 \sin \lambda z e^{\sigma t}, \end{aligned} \right\} \dots \dots \dots (2.5)$$

where u_1 , v_1 and w_1 are functions of r only.

Eliminating p between (2.0) and (2.2) equations (2.0) (2.1) (2.2) and (2.3) reduce to

$$\frac{u_1}{r} + \frac{\partial u_1}{\partial r} + \lambda w_1 = 0, \dots \dots \dots (2.6)$$

$$\nu\left(\nabla_1^2 - \frac{1}{r^2} - \lambda^2 - \frac{\sigma}{\nu}\right)v_1 = 2Au_1, \dots \dots \dots (2.7)$$

$$\frac{\nu}{\lambda} \frac{\partial}{\partial r} \left\{ \left(\nabla_1^2 - \lambda^2 - \frac{\sigma}{\nu} \right) w_1 \right\} = -2\left(A + \frac{B}{r^2}\right)v_1 - \nu\left(\nabla_1^2 - \frac{1}{r^2} - \lambda^2 - \frac{\sigma}{\nu}\right)u_1. \dots \dots (2.8)$$

The boundary conditions are

$$u_1 = v_1 = w_1 = 0 \text{ at } r = R_1 \text{ and } r = R_2. \dots \dots \dots (2.9)$$

The fact that there are no terms containing z in these equations shows that the normal modes of disturbance are simple harmonic with respect to z , the wave-length being $2\pi/\lambda$. σ is a quantity which determines the rate of increase in a normal disturbance. If σ is positive the disturbance increases and the motion is unstable. If σ is negative the disturbance decreases and the motion is stable. If σ is zero the motion is neutral. It will be seen from the way in which σ enters into the equations that it cannot be imaginary or complex unless u_1, v_1, w_1 are complex.

Bessel Functions used in the Solution.

The solution of equations (2.6), (2.7) and (2.8) is developed by means of a type of BESSEL functions of order 1 which vanish at $r = R_1$ and $r = R_2$. Let $J_1(\kappa_s r)$ and $W_1(\kappa_s r)$ be two independent solutions of the BESSEL equation,

$$\left(\nabla_1^2 + \kappa_s^2 - \frac{1}{r^2}\right)f = 0. \dots \dots \dots (3.0)$$

The general solution of (3.0) is

$$f = C_1 J_1(\kappa_s r) + C_2 W_1(\kappa_s r), \dots \dots \dots (3.01)$$

where C_1 and C_2 are constants.

Let us now choose C_1 and C_2 so that f vanishes at $r = R_1$ and $r = R_2$; we then obtain two equations which suffice to determine C_1/C_2 and

The equation for κ_s is

$$\frac{J_1(\kappa_s R_1)}{W_1(\kappa_s R_1)} = \frac{J_1(\kappa_s R_2)}{W_1(\kappa_s R_2)} \dots \dots \dots (3.10)$$

Let the roots of this equation be $\kappa_1, \kappa_2, \kappa_3 \dots$ in ascending order of magnitude. The equation for C_1/C_2 is

$$-\frac{C_2}{C_1} = \frac{J_1(\kappa_s R_1)}{W_1(\kappa_s R_2)} \dots \dots \dots (3.11)$$

Writing $B_1(\kappa_s r)$ for

$$C_1 J_1(\kappa_s r) + C_2 W_1(\kappa_s r), \dots \dots \dots (3.12)$$

and $B_0(\kappa_s r)$ for the corresponding BESSEL function of zero order, namely,

$$B_0(\kappa_s r) = C_1 J_0(\kappa_s r) + C_2 W_0(\kappa_s r), \dots \dots \dots (3.13)$$

we notice that

$$\frac{1}{\kappa_s} \frac{\partial}{\partial r} B_0(\kappa_s r) = -B_1(\kappa_s r), \dots \dots \dots (3.14)$$

and that $B_0(\kappa_s r)$ does not vanish at R_1 and R_2 .

In order to develop any function of r in BESSEL-FOURIER expansions valid between the limits R_1 and R_2 the following formulæ will be used* :—

$$\int_{R_1}^{R_2} J_n(\kappa_s r) J_n(\kappa_t r) r dr = \frac{R_2}{\kappa_s^2 - \kappa_t^2} \{ \kappa_t J_n(\kappa_s R_2) J'_n(\kappa_t R_2) - \kappa_s J_n(\kappa_t R_2) J'_n(\kappa_s R_2) \} \\ - \frac{R_1}{\kappa_s^2 - \kappa_t^2} \{ \kappa_t J_n(\kappa_s R_1) J'_n(\kappa_t R_1) - \kappa_s J_n(\kappa_t R_1) J'_n(\kappa_s R_1) \} \quad (3.20)$$

and

$$\int_{R_1}^{R_2} J_n^2(\kappa_s r) r dr = \frac{R_2^2}{2} \left\{ J_n'^2(\kappa_s R_2) + \left(1 - \frac{n^2}{\kappa_s^2 R_2^2} \right) J_n^2(\kappa_s R_2) \right\} \\ - \frac{R_1^2}{2} \left\{ J_n'^2(\kappa_s R_1) + \left(1 - \frac{n^2}{\kappa_s^2 R_1^2} \right) J_n^2(\kappa_s R_1) \right\}, \quad (3.21)$$

where $J_n(\kappa_s r)$ is any BESSEL function of order n , and κ_s and κ_t may be real or complex numbers. Particular cases of (3.20) and (3.21) when $n = 0$ and $n = 1$ and κ_s and κ_t are roots of (3.10) are

$$\int_{R_1}^{R_2} B_0(\kappa_s r) B_0(\kappa_t r) r dr = 0, \quad (3.22)$$

$$\int_{R_1}^{R_2} B_1(\kappa_s r) B_1(\kappa_t r) r dr = 0, \quad (3.23)$$

$$\int_{R_1}^{R_2} B_0^2(\kappa_s r) r dr = \frac{1}{2} \{ R_2^2 B_0^2(\kappa_s R_2) - R_1^2 B_0^2(\kappa_s R_1) \} = H_s, \quad (3.24)$$

$$\int_{R_1}^{R_2} B_1^2(\kappa_s r) r dr = \frac{1}{2} \{ R_2^2 B_1^2(\kappa_s R_2) - R_1^2 B_1^2(\kappa_s R_1) \} = H_s, \quad (3.25)$$

Any continuous function $f(r)$ of r which vanishes at R_1 and R_2 may be developed in a BESSEL-FOURIER series

$$f(r) = \sum_{s=1}^{\infty} a_s B_1(\kappa_s r) \quad (3.30)$$

This series is valid between the limits R_1 and R_2 and

$$a_s = \frac{1}{H_s} \int_{R_1}^{R_2} f(r) B_1(\kappa_s r) r dr \quad (3.31)$$

On the other hand any continuous function $F(r)$ of r may be developed in a BESSEL-FOURIER series

$$F(r) = b_0 + \sum_{s=1}^{\infty} b_s B_0(\kappa_s r) \quad (3.32)$$

* GRAY and MATHEWS, 'BESSEL Functions,' p. 53.

This series is also valid between the limits R_1 and R_2 and

$$b_s = \frac{1}{H_s} \int_{R_1}^{R_2} F(r) B_0(\kappa_s r) r dr. \dots \dots \dots (3.33)$$

It will be noticed that a constant term occurs in (3.32). At first sight this appears surprising. In most BESSEL-FOURIER expansions this extra term does not appear because it is possible to express a constant as a BESSEL-FOURIER expansion containing all the other terms. In the case of the expansion (3.32) it will be found that it is not possible to do this. The functions $B_0(\kappa_1 r)$, $B_0(\kappa_2 r)$, . . . do not form a complete set of normal functions without the constant.

Development of Solution of (2.6), (2.7) and (2.8) in Bessel Functions.

It is found convenient to express u_1 , v_1 and w_1 as series of types (3.30) and (3.32) because when these series are introduced into the equations (2.6), (2.7) and (2.8) they yield linear relations between the coefficients of the various expansions. At the same time the form (3.30) is specially convenient because a series of that form automatically satisfies the boundary conditions at R_1 and R_2 .

Integral of (2.7).

Assume the following series for u_1

$$u_1 = \sum_{m=1}^{\infty} \alpha_m B_1(\kappa_m r). \dots \dots \dots (4.0)$$

This satisfies the conditions $u_1 = 0$ at R_1 and R_2 . Substituting this in equation (2.7) it will be seen that the complete solution of (2.7) is

$$v_1 = C_3 J_1(i\lambda' r) + C_4 (i\lambda' r) + \sum_{m=1}^{\infty} b_m B_1(\kappa_m r), \dots \dots \dots (4.10)$$

where i is $\sqrt{-1}$ and C_3 and C_4 are the two arbitrary constants occurring in the complementary function

$$\lambda'^2 = \lambda^2 + \sigma/\nu \dots \dots \dots (4.11)$$

and

$$b_m = -\frac{2A\alpha_m}{\nu(\kappa_m^2 + \lambda^2 + \sigma/\nu)}. \dots \dots \dots (4.12)$$

The boundary condition $v_1 = 0$ at R_1 and R_2 gives

$$C_3 = C_4 = 0. \dots \dots \dots (4.13)$$

Integral of (2.8).

The complete solution of the equation (2.8) may be written in the form

$$w_1 = C_5 + C_6 J_0(i\lambda'r) + C_7 W_0(i\lambda'r) + \sum_{m=1}^{\infty} c_m B_0(\kappa_m r), \dots \dots \dots (4.20)$$

where C_5, C_6, C_7 are the three arbitrary constants which occur in the complementary function—that is, in the solution of

$$\frac{\nu}{\lambda} \frac{\partial}{\partial r} \left(\nabla_1^2 - \lambda^2 - \frac{\sigma}{\nu} \right) w_1 = 0, \dots \dots \dots (4.201)$$

$J_0(i\lambda'r)$ and $W_0(i\lambda'r)$ are two independent solutions of

$$(\nabla_1^2 - \lambda'^2) J_0(i\lambda'r) = 0.$$

Substituting (4.20) in (2.8) the following equation is obtained to determine the coefficients c_m

$$\sum_{m=1}^{\infty} \frac{\nu}{\lambda} (\kappa_m^2 + \lambda'^2) c_m \frac{\partial}{\partial r} B_0(\kappa_m r) = 2 \left(A + \frac{B}{r^2} \right) \sum_{m=1}^{\infty} b_m B_1(\kappa_m r) - \nu \sum_{m=1}^{\infty} (\kappa_m^2 + \lambda'^2) \alpha_m B_1(\kappa_m r). \dots \dots (4.21)$$

Substituting for b_m from (4.12) and using the relation

$$\frac{\partial}{\partial r} B_0(\kappa_m r) = -\kappa_m B_1(\kappa_m r)$$

(4.21) becomes

$$\sum_{m=1}^{\infty} c_m \left(\frac{\nu \kappa_m}{\lambda} \right) (\lambda'^2 + \kappa_m^2) B_1(\kappa_m r) = \sum_{m=1}^{\infty} \nu (\kappa_m^2 + \lambda'^2) \alpha_m B_1(\kappa_m r) + 2 \left(A + \frac{B}{r^2} \right) \sum_{m=1}^{\infty} \frac{2A\alpha_m}{\nu (\kappa_m^2 + \lambda'^2)} B_1(\kappa_m r). \dots \dots (4.22)$$

Treatment of the Equation of Continuity (2.6).

Substituting for u_1 from (4.0) and for w_1 from (4.20)

$$\frac{u_1}{r} + \frac{\partial u_1}{\partial r} \text{ becomes } \sum \kappa_m \alpha_m B_0(\kappa_m r), \dots \dots \dots (4.30)$$

so that (2.6) becomes

$$0 = \sum (\kappa_m \alpha_m + \lambda c_m) B_0(\kappa_m r) + \lambda \{ C_5 + C_6 J_0(i\lambda'r) + C_7 W_0(i\lambda'r) \}. \dots \dots (4.31)$$

In order that we may equate coefficients of $B_0(\kappa_m r)$ for all values of m it is necessary to expand the terms inside the second bracket in (4.31) in a BESSEL-FOURIER series of the form (3.32).

Expansion of $C_5 + C_6 J_0(i\lambda'r) + C_7 W_0(i\lambda'r)$.

Let

$$C_5 + C_6 J_0(i\lambda'r) + C_7 W_0(i\lambda'r) = C'_5 + \sum_{m=1}^{\infty} d_m B_0(\kappa_m r), \dots \dots \dots (4.40)$$

then from (3.33)

$$d_m = \frac{1}{H_m} \int_{R_1}^{R_2} B_0(\kappa_m r) \{C_6 J_0(i\lambda'r) + C_7 W_0(i\lambda'r)\} r dr. \dots \dots \dots (4.41)$$

This integral is a particular case of (3.20). Remembering that

$$B'_0(\kappa_m R_1) = B'_0(\kappa_m R_2) = 0,$$

it will be seen from (3.20) that

$$d_m = \frac{-i\lambda'}{H_m(\kappa_m^2 + \lambda'^2)} \left[\begin{array}{l} C_6 \{R_2 B_0(\kappa_m R_2) J'_0(i\lambda'R_2) - R_1 B_0(\kappa_m R_1) J'_0(i\lambda'R_1)\} \\ + C_7 \{R_2 B_0(\kappa_m R_2) W'_0(i\lambda'R_2) - R_1 B_0(\kappa_m R_1) W'_0(i\lambda'R_1)\} \end{array} \right]. \dots \dots \dots (4.42)$$

The constant term is

$$C'_5 = C_5 + \frac{2i}{(R_1^2 - R_2^2)\lambda'} [C_6 \{R_2 J'_0(i\lambda'R_2) - R_1 J'_0(i\lambda'R_1)\} + C_7 \{R_2 W'_0(i\lambda'R_2) - R_1 W'_0(i\lambda'R_1)\}] \dots \dots \dots (4.43)$$

Writing

$$C'_6 = i\lambda'R_2 \{C_6 J'_0(i\lambda'R_2) + C_7 W'_0(i\lambda'R_2)\}, \dots \dots \dots (4.44)$$

$$C'_7 = -i\lambda'R_1 \{C_6 J'_0(i\lambda'R_1) + C_7 W'_0(i\lambda'R_1)\}. \dots \dots \dots (4.45)$$

The expansion may now be written

$$C_5 + C_6 J_0(i\lambda'r) + C_7 W_0(i\lambda'r) = C'_5 + C'_6 \sum_{m=1}^{\infty} \frac{B_0(\kappa_m R_2)}{H_m(\kappa_m^2 + \lambda'^2)} B_0(\kappa_m r) + C'_7 \sum_{m=1}^{\infty} \frac{B_0(\kappa_m R_1)}{H_m(\kappa_m^2 + \lambda'^2)} B_0(\kappa_m r). \dots \dots \dots (4.46)$$

Since C_5 , C_6 and C_7 are entirely arbitrary constants, and the coefficients of C'_6 and C'_7 are independent functions of r , we can regard the right-hand side of (4.46) as being the complementary function of (4.201), the three arbitrary constants now being C'_5 , C'_6 and C'_7 .

We are now in a position to make effective use of the equation of continuity (4.31). Substituting (4.46) in (4.31) we can equate coefficients of $B_0(\kappa_m r)$. In this way

$$\left. \begin{array}{l} C'_5 = 0 \\ \text{and} \dots \dots \dots \\ 0 = \frac{\kappa_m a_m}{\lambda} + c_m + C'_6 \frac{B_0(\kappa_m R_2)}{H_m(\kappa_m^2 + \lambda'^2)} + C'_7 \frac{B_0(\kappa_m R_1)}{H_m(\kappa_m^2 + \lambda'^2)}. \end{array} \right\} \dots \dots \dots (4.47)$$

These equations give c_m in terms of a_m and C'_6 and C'_7 .

Equations for Determining Coefficients a_m .

Next substitute in (4.22) the value of c_m given by (4.47).

There results an equation containing only $a_1, a_2, \dots, a_m, \dots$ and C'_6 and C'_7 . It is not possible, however, to equate coefficients of $B_1(\kappa_m r)$, directly on account of the factor $A+B/r^2$ which occurs on the right-hand side. In order to equate coefficients it is necessary to expand every term of type $(A+B/r^2) B_1(\kappa_m r)$ in a BESSEL-FOURIER series of type (3.30).

Let

$$(A+B/r^2) B_1(\kappa_m r) = {}_1c_m B_1(\kappa_1 r) + {}_2c_m B_1(\kappa_2 r) + \dots + {}_s c_m B_1(\kappa_s r), \dots \quad (4.50)$$

so that

$${}_s c_m = \frac{1}{H_s} \int_{R_1}^{R_2} (A+B/r^2) B_1(\kappa_m r) B_1(\kappa_s r) r dr. \dots \quad (4.51)$$

Substituting these series in (4.22) and also substituting for c_m from (4.47), (4.22) becomes

$$\begin{aligned} - \sum_{m=1}^{\infty} \left\{ \left(\frac{\nu \kappa_m}{\lambda} \right) (\lambda'^2 + \kappa_m^2) \left(C'_6 \frac{B_0(\kappa_m R_2)}{H_m(\kappa_m^2 + \lambda'^2)} + C'_7 \frac{B_0(\kappa_m R_1)}{H_m(\kappa_m^2 + \lambda'^2)} + \frac{\kappa_m \alpha_m}{\lambda} \right) + \nu (\kappa_m^2 + \lambda'^2) \alpha_m \right\} B_1(\kappa_m r) \\ = 4A \sum_{m=1}^{\infty} \left(\frac{\alpha_m}{\nu (\kappa_m^2 + \lambda'^2)} \sum_{s=1}^{\infty} {}_s c_m B_1(\kappa_s r) \right). \dots \quad (4.52) \end{aligned}$$

We can now equate coefficients of $B_1(\kappa_m r)$ in (4.52). The result is

$$\begin{aligned} 0 = \frac{4A}{\nu} \left[\frac{\alpha_{1m} c_1}{\kappa_1^2 + \lambda'^2} + \frac{\alpha_{2m} c_2}{\kappa_2^2 + \lambda'^2} + \frac{\alpha_{3m} c_3}{\kappa_3^2 + \lambda'^2} + \dots \right] \\ + C'_6 \frac{\nu \kappa_m}{\lambda H_m} B_0(\kappa_m R_2) + C'_7 \frac{\nu \kappa_m}{\lambda H_m} B_0(\kappa_m R_1) + \frac{\nu}{\lambda^2} (\kappa_m^2 + \lambda^2) (\kappa_m^2 + \lambda'^2) \alpha_m. \dots \quad (4.53) \end{aligned}$$

We have now a system of linear equations connecting $a_1, a_2, \dots, a_m, C'_6$ and C'_7 . It will be noticed that there are two more unknowns than there are equations. There are, however, two more conditions of which no account has yet been taken which must be satisfied by the solution: w_1 must vanish at R_1 and at R_2 .

Using the equation of continuity (2.6) it will be seen from (4.30) that the conditions that w_1 vanishes at R_1 and R_2 are

$$\sum_{m=1}^{\infty} \kappa_m \alpha_m B_0(\kappa_m R_1) = 0 \dots \quad (4.54)$$

and

$$\sum_{m=1}^{\infty} \kappa_m \alpha_m B_0(\kappa_m R_2) = 0. \dots \quad (4.55)$$

Determination of σ .

We have now used all the boundary conditions and differential equations available. We have also the same number of equations as unknowns, and since the equations are homogeneous, all the unknowns can be eliminated from them. The resulting equation takes the form of an infinite determinant equated to zero. It can be regarded as an equation to determine σ . It is

$$\begin{vmatrix}
 0 & 0 & \kappa_1 B_0(\kappa_1 R_1) & \kappa_2 B_0(\kappa_2 R_1) & \kappa_3 B_0(\kappa_3 R_1) & \dots \\
 0 & 0 & \kappa_1 B_0(\kappa_1 R_2) & \kappa_2 B_0(\kappa_2 R_2) & \kappa_3 B_0(\kappa_3 R_2) & \dots \\
 \frac{\nu^2 \kappa_1}{4A\lambda H_1} B_0(\kappa_1 R_1), & \frac{\nu^2 \kappa_1}{4A\lambda H_1} B_0(\kappa_1 R_2), & \frac{\nu^2}{4A\lambda^2} (\kappa_1^2 + \lambda^2) (\kappa_1^2 + \lambda'^2) + \frac{{}_1C_1}{\kappa_1^2 + \lambda'^2}, & \dots & \dots & \dots \\
 \frac{\nu^2 \kappa_2}{4A\lambda H_2} B_0(\kappa_2 R_1), & \frac{\nu^2 \kappa_2}{4A\lambda H_2} B_0(\kappa_2 R_2), & \frac{{}_2C_1}{\kappa_1^2 + \lambda'^2} & \frac{\nu^2}{4A\lambda^2} (\kappa_2^2 + \lambda^2) (\kappa_2^2 + \lambda'^2) + \frac{{}_2C_2}{\kappa_2^2 + \lambda'^2}, & \dots & \dots \\
 \dots & \dots & \dots & \dots & \dots & \dots
 \end{vmatrix} \quad (4.60)$$

This may be written

$$\begin{vmatrix}
 0 & 0 & \kappa_1 (\kappa_1^2 + \lambda'^2) B_0(\kappa_1 R_1), & \kappa_2 (\kappa_2^2 + \lambda'^2) B_0(\kappa_2 R_1) & \dots & \dots \\
 0 & 0 & \kappa_1 (\kappa_1^2 + \lambda'^2) B_0(\kappa_1 R_2), & \kappa_2 (\kappa_2^2 + \lambda'^2) B_0(\kappa_2 R_2) & \dots & \dots \\
 0 = \Delta_1 = \frac{\kappa_1}{H_1} B_0(\kappa_1 R_1), & \frac{\kappa_1}{H_1} B_0(\kappa_1 R_2), & {}_1L'_1 & {}_1C_2 & \dots & \dots \\
 \frac{\kappa_2}{H_2} B_0(\kappa_2 R_1), & \frac{\kappa_2}{H_2} B_0(\kappa_2 R_2), & {}_2C_1 & L'_2 & \dots & \dots \\
 \dots & \dots & \dots & \dots & \dots & \dots
 \end{vmatrix} \quad (4.61)$$

Where

$$L'_m = \frac{\nu^2}{4A\lambda^2} (\kappa_m^2 + \lambda^2) (\kappa_m^2 + \lambda'^2)^2 + {}_mC_m, \quad (4.62)$$

Δ_1 is written to represent the whole determinant, and $\frac{\sigma}{\nu} = \lambda'^2 - \lambda^2$.

Stability of Symmetrical Disturbances.

Equation (4.61) may be regarded as a criterion for the stability of given initial disturbances of the type specified by equations (2.5). If the value of σ determined from (4.61) is real, then the motion is stable or unstable according as σ is negative or positive. If σ is complex the motion is unstable if the real part of σ is positive. The motion is then an oscillation of increasing amplitude. A complete discussion of stability necessitates a search for complex roots of (4.61) as well as real ones.

Reasoning on the lines of RAYLEIGH'S analogy it will be noticed that the type of instability which ensues when a liquid whose density increases with height is disturbed from its position of unstable equilibrium cannot be an oscillation of increasing amplitude. Though RAYLEIGH'S analogy cannot be applied without modification to viscous fluids, it seems unlikely that unstable oscillations of this type can exist when the disturbance is symmetrical. It will be seen moreover in Part II, that careful experiments over a wide range of speeds have failed to detect them. It does not seem worth while, therefore, to embark on the extremely laborious and difficult work which a search for complex roots of (4.61) would entail. I have, therefore, limited the work which follows to a discussion of the real roots of (4.61).

Direction in which it is Profitable to Continue the Discussion of (4.61).

The object with which this work was undertaken was to search for a mathematical solution of some case of fluid instability which can conveniently be subjected to experimental investigation.

It is known that all possible types of steady motion of a viscous fluid are stable at very low speeds.* If, therefore, one is examining experimentally the stability of any type of steady motion which is dynamically possible at all speeds, it is convenient, in carrying out the experiment, to start the flow at a slow speed and to increase the speed slowly. If the motion is ever unstable it will become so at some definite speed, and the experiment would naturally involve measuring that speed. The instability which then sets in is that particular type of instability which occurs at the lowest speed, and evidently for this type of instability $\sigma = 0$.

If σ be put equal to 0, so that $\lambda = \lambda'$, (4.61) may be regarded as an equation giving the point at which instability will first appear when the speed of the initial steady motion is slowly increased. Equation (4.61), however, gives us more information than that. Up to the present the wave length of the disturbance which is equal to $2\pi/\lambda$ has been considered as entirely arbitrary. Equation (4.61) determines the speed at which instability of arbitrary wave-length λ first appears. One particular value of λ will correspond with the minimum speed at which instability can appear. In experiments made with viscous fluids this value would be the one which would be observed

* RAYLEIGH "On the Motion of a Viscous Fluid," 'Phil. Mag.,' 1913, vol. 26, pp. 776-786.

when the instability first appeared. Probably it is the only one which could ever be observed.

It will be seen that equation (4.61) can therefore be used to predict the dimensions and form of the disturbance as well as the speed at which it will appear. Accordingly in the numerical work which follows, when $\sigma = 0$ (4.61) is regarded as an equation in two variables. The ratio of the speed of the outer cylinder to that of the inner is regarded as a constant, μ ; the speed of the flow is then proportional at all points to the speed of the inner cylinder, Ω_1 , which is taken as one of the variables. This enters into the equation in the quantities A and c_s . The other variable is λ . To determine the instability which will first appear with any particular value of μ , *i.e.*, Ω_2/Ω_1 , various values of λ are inserted in (4.61) and the one which yields the minimum value of Ω_1 is taken.

To prove that the steady motion is unstable at slightly higher speeds, and stable, so far as real roots of (4.61) are concerned, at slightly lower speeds of the cylinders, it is necessary to show that a slight increase in Ω_1 gives rise to a small positive value of σ , while a slight decrease in Ω_1 gives rise to a small negative value. It is shown later that this is the case.*

Approximate Formulae.

If any particular values of R_1 and R_2 be taken, and also a particular value of μ , it would certainly be possible to find the corresponding numerical values of Ω_1 and λ from (4.61). The labour involved would, however, be so great that it might take months to perform the computation in a single case. To complete the investigation would necessitate finding solutions for various values of R_2/R_1 and for a complete range of μ from large negative to large positive values.

These considerations show that it would be practically impossible to undertake a complete numerical discussion of the problem. On the other hand it will be shown in the second part of this paper that the dimensions of the apparatus which was constructed to investigate the problem, impose a limitation on the range of ratios R_2/R_1 with which it is possible to perform satisfactory experiments. In that apparatus it was found that if the radius of the inner cylinder was much less than half that of the outer one, effects due to the ends of the apparatus began to be appreciable and difficult to eliminate, so that the initial motion ceased to be the same as that between two infinite cylinders. Most of the experiments were therefore conducted with cylinders for which $R_2 - R_1$ was considerably smaller than either R_1 or R_2 , that is to say the thickness of the space between the cylinders was small compared with their radii.

Under these conditions it is possible to reduce (4.61) to an approximate form which can be used effectively for numerical calculation. Writing d for $R_2 - R_1$ the work can conveniently be carried to the second approximation, so as to include small terms involving the first power of d/R_1 , but not those involving $(d/R_1)^2$.

* See p. 311.

Approximate Expressions for $B_0(\kappa_m r)$ and $B_1(\kappa_m r)$.

Writing $\kappa_m r = x$ it will readily be seen that in order that $B_1(\kappa_m r)$ may vanish at $r = R_1$ and $r = R_2$ when d/R_1 is small x must be a large number. Hence the ordinary asymptotic expressions for BESSEL functions can be used.

The asymptotic expansions used are correct to the second approximation, *i.e.*, they include terms in $1/x$ but not terms in $1/x^2$. They are*

$$\left. \begin{aligned} \sqrt{\frac{1}{2}\pi x} J_0(x) &= \cos\left(x - \frac{\pi}{4}\right) + \frac{1}{8x} \sin\left(x - \frac{\pi}{4}\right), \\ \sqrt{\frac{1}{2}\pi x} W_0(x) &= \sin\left(x - \frac{\pi}{4}\right) - \frac{1}{8x} \cos\left(x - \frac{\pi}{4}\right), \\ \sqrt{\frac{1}{2}\pi x} J_1(x) &= \sin\left(x - \frac{\pi}{4}\right) + \frac{3}{8x} \cos\left(x - \frac{\pi}{4}\right), \\ \sqrt{\frac{1}{2}\pi x} W_1(x) &= -\cos\left(x - \frac{\pi}{4}\right) + \frac{3}{8x} \sin\left(x - \frac{\pi}{4}\right). \end{aligned} \right\} \dots \dots \dots (5.0)$$

Let

$$\sqrt{\kappa_m} B_1(x) = \{C'_1 J_1(x) + C'_2 W_1(x)\} \sqrt{\frac{1}{2}\pi}, \dots \dots \dots (5.11)$$

and let the constants C'_1 and C'_2 be chosen so that

$$\sqrt{\kappa_m} B_1(x) = (x)^{-\frac{1}{2}} \sin(x - \frac{1}{4}\pi + \epsilon'). \dots \dots \dots (5.12)$$

Then from (5.0)

$$\left. \begin{aligned} C'_1 + \frac{3}{8x} C'_2 &= \cos \epsilon' \\ -C'_2 + \frac{3}{8x} C'_1 &= \sin \epsilon'. \end{aligned} \right\} \dots \dots \dots (5.13)$$

Solving (5.13) and neglecting terms in $1/x^2$ ϵ' can be regarded as constant over the range of values of x corresponding with the space between the cylinders, and the following expressions are obtained for C'_1 and C'_2

$$C'_1 = \cos \epsilon' + \frac{3}{8x} \sin \epsilon', \quad C'_2 = -\sin \epsilon' + \frac{3}{8x} \cos \epsilon'. \dots \dots \dots (5.14)$$

To find the corresponding expression for $B_0(x)$, note that

$$\sqrt{\kappa_m} B_0(x) = \{C'_1 J_0(x) + C'_2 W_0(x)\} \sqrt{\frac{1}{2}\pi},$$

substituting from (5.14) and (5.0)

$$\sqrt{\kappa_m} B_0(x) = x^{-\frac{1}{2}} \left\{ \cos\left(x - \frac{1}{4}\pi + \epsilon'\right) + \frac{1}{2x} \sin\left(x - \frac{1}{4}\pi + \epsilon'\right) \right\}. \dots \dots \dots (5.15)$$

* See JAHNKE and EMDE, "Functionen Tafeln," p. 99.

Next replace x by $\kappa_m r$ and put $r = R_1 + y$. y is then the distance of any point from the inner cylinder. Choose ϵ' so that

$$\kappa_m R_1 - \frac{1}{4}\pi + \epsilon' = 0. \quad (5.16)$$

$B_1(\kappa_m r)$ then vanishes at $r = R_1$, and (5.12) becomes

$$B_1(\kappa_m r) = (R_1 + y)^{-\frac{1}{2}} \sin \kappa_m y, \quad (5.17)$$

and (5.15) becomes

$$B_0(\kappa_m r) = (R_1 + y)^{-\frac{1}{2}} \left\{ \cos \kappa_m y + \frac{1}{2(R_1 + y)\kappa_m} \sin \kappa_m y \right\}. \quad (5.18)$$

The values of κ_m are found by putting $B_1(\kappa_m R_2) = 0$, i.e., $\sin(\kappa_m d) = 0$. Hence evidently

$$\kappa_m = m\pi/d, \quad (5.20)$$

where m is a positive integer. The successive values of κ_m are

$$\pi/d, \quad 2\pi/d, \quad 3\pi/d, \dots$$

Writing κ for π/d so that $\kappa_m = m\kappa$ the asymptotic expression for the BESSEL functions up to and including first order small terms are

$$B_1(\kappa_m r) = (R_1 + y)^{-\frac{1}{2}} \sin m\kappa y, \quad (5.21)$$

$$B_0(\kappa_m r) = (R_1 + y)^{-\frac{1}{2}} \{ \cos m\kappa y + [2m\kappa(y + R_1)]^{-1} \sin m\kappa y \}. \quad (5.22)$$

It will be noticed that if we had attempted to proceed beyond the second approximation it would not have been found that $\kappa_m = m\kappa$, and the work would have been much more complicated.

Approximate Expressions for the Terms in (4.61).

In the first two rows of the determinant we can replace

$$B_0(\kappa_m R_1) \text{ by } (R_1)^{-\frac{1}{2}} \text{ and } B_0(\kappa_m R_2) \text{ by } (-1)^m R^{-\frac{1}{2}}. \quad (5.30)$$

$\kappa_m = m\kappa$ and λ' is the same as λ since $\sigma = 0$.

In the first two columns of (4.61) appears H_m . From (5.30) and (3.24)

$$H_m = \frac{1}{2}(R_2 - R_1) = \frac{1}{2}d. \quad (5.31)$$

It remains to find the approximate expressions for ${}_s c_m$ and L'_m . At this stage some care is necessary. On referring to equation (4.51) it will be seen that ${}_s c_m$ is an integral containing the expression $A + B/r^2$ which represents the angular velocity of any annulus of liquid in the undisturbed state. When d is small compared with R_1 and when neither Ω_1 nor Ω_2 are very large the quantities A and B/r^2 are both large and nearly equal in magnitude, but of opposite sign. For this reason therefore it is necessary to express $A + B/r^2$ in terms of Ω_1, μ, d and R_1 . This has been done, the expansion being

carried to the second approximation was to include terms containing the first power of d/R_1 . It is

$$A + B/r^2 = \Omega_1 \left\{ 1 - \frac{y}{d} (1 - \mu) \left(1 + \frac{3d}{2R_1} \right) + \frac{3}{2} \frac{y^2}{d^2} (1 - \mu) \frac{d}{R_1} \right\}, \dots \dots (5.32)$$

where $\mu = R_2/R_1$.

This expression is now substituted in (4.51) which becomes

$${}_s c_m = \frac{1}{H_s} \int_0^d \left(\alpha + \beta \frac{y}{d} + \gamma \frac{y^2}{d^2} \right) \sin m\kappa y \sin s\kappa y \kappa dy, \dots \dots (5.33)$$

where

$$\alpha = \frac{\Omega_1}{\kappa}, \quad \beta = -\frac{\Omega_1}{\kappa} (1 - \mu) \left(1 + \frac{3}{2} \frac{d}{R_1} \right), \quad \gamma = \frac{3}{2} \frac{\Omega_1 d}{\kappa R_1} (1 - \mu). \dots \dots (5.34)$$

Let $\kappa y = \eta$, then

$${}_s c_m = \frac{1}{H_s} \int_0^\pi \left(\alpha + \beta \frac{\eta}{\pi} + \gamma \frac{\eta^2}{\pi^2} \right) \sin m\eta \sin s\eta d\eta. \dots \dots (5.35)$$

If s is not equal to m

$$\left. \begin{aligned} \int_0^\pi \sin m\eta \sin s\eta d\eta &= 0, \\ \int_0^\pi \eta \sin m\eta \sin s\eta d\eta &= 0, \text{ when } m+s \text{ is even,} \\ &= \frac{-4ms}{(m^2 - s^2)^2}, \text{ when } m+s \text{ is odd,} \\ \int_0^\pi \eta^2 \sin m\eta \sin s\eta d\eta &= \frac{4\pi ms}{(m^2 - s^2)^2}, m+s \text{ even,} \\ &= \frac{-4\pi ms}{(m^2 - s^2)^2}, m+s \text{ odd.} \end{aligned} \right\} \dots \dots (5.36)$$

If $s = m$

$$\left. \begin{aligned} \int_0^\pi \sin^2 m\eta d\eta &= \frac{1}{2}\pi, \\ \int_0^\pi \eta \sin^2 m\eta d\eta &= \frac{1}{4}\pi^2, \\ \int_0^\pi \eta^2 \sin^2 m\eta d\eta &= \frac{\pi^3}{3} - \frac{\pi}{4m^2}. \end{aligned} \right\} \dots \dots (5.37)$$

Inserting the values of $\alpha, \beta, \gamma, H_m$, it will be found after some reduction that

$$\left. \begin{aligned} {}_s c_m &= \frac{8ms\Omega_1 (1 - \mu)}{(m^2 - s^2)^2 \pi^2}, m+s \text{ odd,} \\ {}_s c_m &= \frac{8ms\Omega_1 (1 - \mu)}{(m^2 - s^2)^2 \pi^2} \left(\frac{3d}{2R_1} \right), m+s \text{ even,} \\ {}_m c_m &= \frac{1}{2}\Omega_1 (1 + \mu) - \Omega_1 (1 - \mu) \frac{d}{R_1} \left(\frac{1}{4} + \frac{3}{4m^2\pi^2} \right). \end{aligned} \right\} \dots \dots (5.38)$$

and

Approximate Expression for Determinant.

On replacing the terms in the first two columns and the first two rows of the determinant Δ_1 by their approximate values, some reductions can be made immediately. The first column can be divided by $2\kappa d^{-1}R_1^{-\frac{1}{2}}$, the second by $2\kappa d^{-1}R_2^{-\frac{1}{2}}$, the first row by $\kappa^3 R_1^{-\frac{1}{2}}$ and the second by $\kappa^3 R_2^{-\frac{1}{2}}$. If θ be written for λ/κ (4.6) becomes

$$0 = \begin{vmatrix} 0 & 0 & 1(1^2 + \theta^2) & 2(2^2 + \theta^2) & 3(3^2 + \theta^2) & \dots \\ 0 & 0 & -1(1^2 + \theta^2) & 2(2^2 + \theta^2) & -3(3^2 + \theta^2) & \dots \\ 1 & -1 & L'_1 & {}_1c_2 & {}_1c_3 & \dots \\ 2 & 2 & {}_2c_1 & L'_2 & {}_2c_3 & \dots \\ 3 & -3 & {}_3c_1 & {}_3c_2 & L'_3 & \dots \\ \dots & \dots & \dots & \dots & \dots & \dots \end{vmatrix} \quad (5.40)$$

Next perform the following operations on this determinant :—

- (1) Divide the $(n+2)^{th}$ column and the $(m+2)^{th}$ row by m .
- (2) Add and subtract the first two rows and the first two columns. This reduces every alternate term to zero.
- (3) Multiply all terms by $\pi^2 \{8\Omega_1(1-\mu)\}^{-1}$ but divide these factors out again from the first two rows and columns. The equation $\Delta_1 = 0$ may now be written.

$$0 = \Delta_2 = \begin{vmatrix} 0 & 0 & 1^2 + \theta^2 & 0 & 3^2 + \theta^2 & \dots \\ 0 & 0 & 0 & 2^2 + \theta^2 & 0 & \dots \\ 1 & 0 & L_1 & \frac{1}{(1^2 - 2^2)^2} & \frac{3d}{2R_1(1^2 - 3^2)^2} & \dots \\ 0 & 1 & \frac{1}{(2^2 - 1^2)^2} & L_2 & \frac{1}{(2^2 - 3^2)^2} & \dots \\ 1 & 0 & \frac{3d}{2R_1(3^2 - 1^2)^2} & \frac{1}{(3^2 - 2^2)^2} & L_3 & \dots \\ 0 & 1 & \frac{1}{(4^2 - 1^2)^2} & \frac{3d}{2R_1(4^2 - 2^2)^2} & \frac{1}{(4^2 - 3^2)^2} & \dots \\ \dots & \dots & \dots & \dots & \dots & \dots \end{vmatrix} \quad (5.41)$$

Where Δ_2 is used as a symbol to represent the determinant and

$$L_m = \frac{\pi^2}{8\Omega_1(1-\mu)m^2} \left\{ \frac{\pi^4 \nu^2 (m^2 + \theta^2)^3}{4Ad^4\theta^2} + \Omega_1 \left(\frac{1+\mu}{2} \right) - (1-\mu) \frac{\Omega_1 d}{R_1} \left(\frac{1}{4} + \frac{3}{4m^2\pi^2} \right) \right\}.$$

Remembering that

$$A = \Omega_1 \left(1 - \frac{R_2^2}{R_1^2} \mu\right) \left(1 - \frac{R_2^2}{R_1^2}\right)^{-1},$$

it will be found that

$$L_m = \frac{\pi^2}{16m^2} \left\{ \frac{1+\mu}{1-\mu} - \frac{d}{R_1} \left(\frac{1}{2} + \frac{3}{2m^2\pi^2} \right) - \frac{P(m^2 + \theta^2)^3}{\theta^2} \right\}, \dots \dots \dots (5.42)$$

where

$$P = \frac{\pi^4 \nu^2 (R_1 + R_2)}{2\Omega_1^2 d^3 R_1^2 (1 - R_2^2 \mu / R_1^2) (1 - \mu)}, \dots \dots \dots (5.43)$$

Since Ω_1 only occurs in Δ_2 through the term P, P may be regarded as the variable. It is required therefore to find the maximum possible value of P consistent with (5.41). To do this it is necessary to insert a number of different trial values of θ in Δ_2 and then to solve (5.41) to find P in each case. The value of θ for which P is a maximum determines the dimensions of the eddies into which the flow will resolve itself when instability sets in. At first sight this seems to be a very complicated piece of work, but it is possible to perform certain operations on Δ_2 which greatly increase the rapidity with which its roots converge to definite values. These operations will now be explained.

Limiting Case when μ is nearly equal to 1.

When μ is nearly equal to 1 the diagonal terms of Δ_2 which contain the factor $(1 - \mu)^{-1}$ become large compared with all the other terms. Consider the determinant obtained by taking the first $m+2$ rows and columns of Δ_2 . If this determinant be expanded each term will contain $m+2$ factors, and the greatest terms will be those containing the maximum number of factors L_m from the diagonal. In the limit when $\mu \rightarrow 1$ these terms will become infinitely great compared with all the others. Since two of the factors of each term must come from the first two rows and two from the first two columns, neither of which contained any of the L_m terms, it follows that no term can contain more than $m-2$ factors of type L_m . The limiting value of the determinant will therefore be found by taking all terms which can be obtained by choosing a term from each of the first two rows, a term from each of the first two columns and $m-2$ diagonal terms.

Each term is of the form

$$\left(\frac{L_1 L_2 \dots L_m}{L_s L_t} \right) (s^2 + \theta^2) (t^2 + \theta^2),$$

where s and t are two integers, one of which is even and the other odd. It is evident therefore that the limiting value of Δ_2 can be expressed in the form

$$\lim_{\mu \rightarrow 1} \Delta_2 = (L_1 L_2 L_3 \dots L_m \dots) \left(\frac{1^2 + \theta^2}{L_1} + \frac{3^2 + \theta^2}{L_3} + \frac{5^2 + \theta^2}{L_5} + \dots \right) \left(\frac{2^2 + \theta^2}{L_2} + \frac{4^2 + \theta^2}{L_4} + \dots \right). \quad (5.50)$$

Evaluation of the Greatest Root of (5.41).

It is clear that the greatest value of P consistent with the equation $\Delta_2 = 0^*$ is the greatest root of the equation

$$\frac{1^2 + \theta^2}{L_1} + \frac{3^2 + \theta^2}{L_3} + \dots = 0. \dots \dots \dots (5.51)$$

Writing

$$P' = \frac{1 - \mu}{1 + \mu} P. \dots \dots \dots (5.52)$$

Neglecting $\frac{d}{R_1} \left(\frac{1 - \mu}{1 + \mu} \right)$ which $\rightarrow 0$ as $\mu \rightarrow 1$ (5.51) becomes

$$\frac{1^2(1^2 + \theta^2)}{1 - \frac{P'}{\theta^2}(1^2 + \theta^2)^3} + \frac{3^2(3^2 + \theta^2)}{1 - \frac{P'}{\theta^2}(3^2 + \theta^2)^3} + \dots = 0. \dots \dots \dots (5.53)$$

For any particular value of θ it is a simple matter to approximate to the greatest root of (5.53), which evidently lies between $P' = \theta^2 (1^2 + \theta^2)^{-3}$ and $P' = \theta^2 (3^2 + \theta^2)^{-3}$. After a few terms the 1 in the denominator becomes small compared with

$$\frac{P'}{\theta^2} (m^2 + \theta^2)^3.$$

Neglecting it, the $\frac{1}{2} (m+1)^{\text{th}}$ term is then

$$- \frac{m^2 \theta^2}{P' (m^2 + \theta^2)^2}.$$

The rest of the series including this term is then

$$- \frac{\theta^2}{P'} \left\{ \frac{m^2}{(m^2 + \theta^2)^2} + \frac{(m+2)^2}{((m+2)^2 + \theta^2)^2} + \dots \right\}. \dots \dots \dots (5.54)$$

After a few more terms it will be possible to neglect the θ^2 which occurs in the denominator of each term. If the first term inside the bracket of (5.54) for which it is possible to do this is

$$\frac{s^2}{(s^2 + \theta^2)^2},$$

the remainder of the series including this term is

$$\frac{1}{s^2} + \frac{1}{(s+2)^2} + \frac{1}{(s+4)^2} + \dots$$

This series can be summed exactly.

Proceeding in this way it was found in a rough calculation that the greatest roots of (5.53) are associated with values of θ^2 in the neighbourhood of 1. Accordingly the

* The greatest root of $\frac{2^2 + \theta^2}{L_2} + \dots = 0$ can easily be shown to be less than the greatest root of (5.51).

values of P' were calculated to three significant figures for the series of values $\theta^2 = 0.8, 0.9, 1.0, 1.1, 1.2$. The corresponding values of P' are 0.0562, 0.0569, 0.0571, 0.0569, 0.0563. The variation of P' with θ is shown in a curve in fig. 2. On

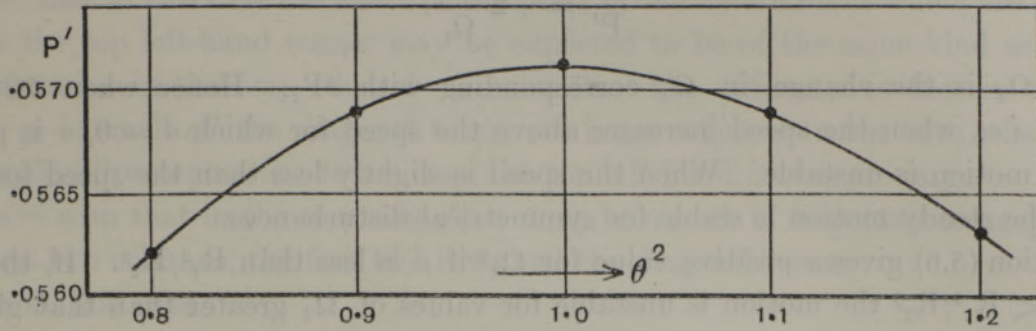


Fig. 2.

looking at that curve it will be seen that the maximum value of P' is 0.0571. It occurs when $\theta^2 = 1.00$. There is no reason to suppose that the correct value of θ^2 is exactly 1, but it almost certainly lies between 0.98 and 1.02.

Stability when the Cylinders are rotating in the same direction with slightly different velocities.

We are now in a position to make some definite predictions about the stability of the flow when μ is nearly 1—that is, when the cylinders are rotating in the same direction with slightly different velocities. In the first place the motion changes from being stable to being unstable when Ω_1 passes through the value given by*

$$\left(\frac{\pi^4 \nu^2 (R_1 + R_2)}{2\Omega_1^2 d^3 R_1^2 (1 - R_2^2 \mu / R_1^2) (1 - \mu)} \right) \left(\frac{1 - \mu}{1 + \mu} \right) = 0.0571. \tag{5.6}$$

It seems evident that at speeds below this the motion must be stable while at higher speeds it must be unstable, but it is perhaps worth while to prove that this is the case by writing down the equation for σ and showing that it changes from a negative to a positive value as Ω_1 increases through the value given by (5.6).

Retaining terms in σ from (4.61) the equation equivalent to (5.53) is

$$0 = \sum_{m \text{ odd}} \frac{m^2 (m^2 + \theta^2 + x)}{1 - \frac{P'}{\theta^2} (m^2 + \theta^2) (m^2 + \theta^2 + x)^2}, \dots \tag{5.61}$$

where $x = \frac{\sigma}{\kappa \nu}$. If P' differs from the value it would have if σ were 0 by a small quantity $\delta P'$, x will also be small and from (5.61) it will be found that

$$x \left[\sum_{m \text{ odd}} \frac{m^2 \left\{ 1 + \frac{P'}{\theta^2} (m^2 + \theta^2)^3 \right\}}{\left\{ 1 - \frac{P'}{\theta^2} (m^2 + \theta^2)^3 \right\}^2} \right] = - \frac{\delta P'}{P'} \left[\sum_{m \text{ odd}} \frac{m^2 (m^2 + \theta^2)}{\left\{ 1 - \frac{P'}{\theta^2} (m^2 + \theta^2)^3 \right\}^2} \right]. \tag{5.62}$$

* From (5.43) and (5.52).

Since the series inside the square brackets are positive when P' is positive, it appears that x is positive when $\delta P'$ is negative. Also from (5.43) and (5.52)

$$\frac{\delta P'}{P'} = -2 \frac{\delta \Omega_1}{\Omega_1},$$

where $\delta \Omega_1$ is the change in Ω_1 corresponding with δP_1 . Hence when $\delta \Omega_1 / \Omega_1$ is positive, *i.e.*, when the speed increases above the speed for which $\sigma = 0$, σ is positive and the motion is unstable. When the speed is slightly less than the speed for which $\sigma = 0$, the steady motion is stable for symmetrical disturbances.

Equation (5.6) gives a positive value for Ω_1^2 if μ is less than R_1^2/R_2^2 . If, therefore, $\Omega_2/\Omega_1 < R_1^2/R_2^2$ the motion is unstable for values of Ω_1 greater than that given by (5.6). If $\Omega_2/\Omega_1 > R_1^2/R_2^2$ the value of Ω_1 given by (5.6) is imaginary and the motion is stable unless a negative root of (5.53) can be found. It is obvious that there are no negative roots of (5.53) because a negative value of P' makes every term in the series on the left-hand side of the equation positive. The sum of the series, therefore, cannot vanish.

Equation (5.6) shows that Lord RAYLEIGH'S criterion for stability of an inviscid fluid is a limiting case of the criterion for a viscous fluid. Lord RAYLEIGH'S criterion was that a fluid would be stable at all speeds if $\Omega_2/\Omega_1 > R_1^2/R_2^2$, and unstable if $\Omega_2/\Omega_1 < R_1^2/R_2^2$. The former of these is equally true for viscous fluids, but the latter is modified in the sense that if $\Omega_2/\Omega_1 < R_1^2/R_2^2$ the motion is unstable only if Ω_1 is greater than the value given by (5.6). It should be noticed that if the analogy on which Lord RAYLEIGH based his theory is strictly adhered to, the case when $\Omega_2/\Omega_1 < R_1^2/R_2^2$ would be unstable at all speeds, even in a viscous fluid; for a heterogeneous fluid in unstable equilibrium under gravity is not more stable when it is viscous than when it is inviscid.

The second prediction which can be made is that in the unstable case the type of instability which will form is periodic along the length of the cylinder, with a wave-length almost exactly equal to twice the thickness of the layer of fluid between the cylinders. This is a consequence of the fact that $\theta = 1$, for the wave-length of the unstable disturbance is $2\pi/\lambda = 2\pi/\kappa\theta = 2d/\theta$ and this is

$$2d \text{ when } \theta = 1. \quad \dots \dots \dots (5.7)$$

It will be shown in the second part of this paper that the symmetrical type of instability does actually occur under experimental conditions, and that both these predictions are verified with considerable accuracy.

Numerical Approximations when $1 - \mu$ is not small.

When $1 - \mu$ is not small the first few diagonal terms may be of the same order of magnitude as the neighbouring terms which are of the form $(m^2 - n^2)^{-2}$, but on passing down the diagonal of Δ_2 the $(m + 2)^{\text{th}}$ term contains a factor of order of magnitude

Pm^4 , while the other terms in the neighbourhood of the diagonal decrease with the factor $(m^2 - n^2)^{-2}$. This is largest when $m - n = 1$, when it is of order m^{-2} . The diagonal terms, therefore, rapidly become very great compared with all other terms. It appears, therefore, that in this case the effect of the parts of the determinant which are situated far from the top left-hand corner may be expected to be of the same kind as that of the same terms in the case when $1 - \mu$ is small. The difference is that in the case when $1 - \mu$ is small *all* the diagonal terms are large, whereas in the case where $1 - \mu$ is not small, all except a few terms near the top left-hand corner are large.

We have seen that in the case when $\mu \rightarrow 1$ no terms are of importance except those in the first two columns, the first two rows and the diagonal terms.

Hence in this case

$$\lim_{\mu \rightarrow 1} \Delta_2 = \begin{vmatrix} 0 & 0 & 1^2 + \theta^2 & 0 & 3^2 + \theta^2 & \dots & \dots \\ 0 & 0 & 0 & 2^2 + \theta^2 & 0 & \dots & \dots \\ 1 & 0 & L_1 & 0 & 0 & \dots & \dots \\ 0 & 1 & 0 & L_2 & 0 & \dots & \dots \\ 1 & 0 & 0 & 0 & L_3 & \dots & \dots \\ \dots & \dots & \dots & \dots & \dots & \dots & \dots \end{vmatrix} \quad (6.00)$$

$$= L_1 L_2 L_3 \dots \left(\frac{1^2 + \theta^2}{L_1} + \frac{3^2 + \theta^2}{L_2} + \dots \right) \left(\frac{2^2 + \theta^2}{L_2} + \frac{4^2 + \theta^2}{L_4} + \dots \right) \dots \quad (6.01)$$

The product form (6.01) of Δ_2 was obtained from (6.00) by direct expansion of Δ_2 , but it might equally well have been obtained by performing the following series of operations on it: Change the signs of the first two columns. Next divide the third column by L_1 , the fourth by L_2 , the fifth by L_3 , ..., etc., then to the first column add the third, fifth, seventh, ..., columns, and to the second the fourth, sixth, eighth, ..., columns, so that

$$\lim_{\mu \rightarrow 1} \Delta_2 = \begin{vmatrix} \frac{1^2 + \theta^2}{L_1} + \frac{3^2 + \theta^2}{L_3} + \dots & 0 & \frac{1^2 + \theta^2}{L_1} & 0 & \frac{3^2 + \theta^2}{L_3} & \dots \\ 0 & \frac{2^2 + \theta^2}{L_2} + \frac{4^2 + \theta^2}{L_4} + \dots & 0 & \frac{2^2 + \theta^2}{L_2} & 0 & \dots \\ 0 & 0 & 1 & 0 & 0 & \dots \\ 0 & 0 & 0 & 1 & 0 & \dots \\ \dots & \dots & \dots & \dots & \dots & \dots \end{vmatrix} \quad (6.02)$$

The effect of all the distant terms is now concentrated in the first two diagonal terms which are the same as those in (6.01).

Downloaded from https://royalsocietypublishing.org/ on 30 January 2025

The same operations may be performed on Δ_2 when $1 - \mu$ is not small. In this case a determinant is obtained which does not reduce to the first two diagonal terms, but, on the other hand, all the other terms contain factors of the form $(m^2 - n^2)^{-2}$. For this reason the determinant derived in this way, which will be called Δ_3 , converges very much more rapidly than Δ_2 .

$$\Delta_3 = \begin{vmatrix} \frac{1^2 + \theta^2}{L_1} + \frac{3^2 + \theta^2}{L_3} + \dots, & 0 & \frac{1^2 + \theta^2}{L_1}, & 0 & \frac{3^2 + \theta^2}{L_3}, & \dots \\ 0 & \frac{2^2 + \theta^2}{L_2} + \frac{4^2 + \theta^2}{L_4} + \dots, & 0 & \frac{2^2 + \theta^2}{L_2}, & 0 & \dots \\ \epsilon \left\{ \frac{1}{L_3(1^2 - 3^2)^2} + \frac{1}{L_5(1^2 - 5^2)^2} + \dots \right\}, & \frac{1}{L_2(1^2 - 2^2)^2} + \frac{1}{L_4(1^2 - 4^2)^2} + \dots, & 1 & \frac{1}{L_2(1^2 - 2^2)^2}, & \frac{\epsilon}{L_3(1^2 - 3^2)^2}, & \dots \\ \frac{1}{L_1(2^2 - 1^2)^2} + \frac{1}{L_3(2^2 - 3^2)^2} + \dots + \epsilon \left\{ \frac{1}{L_4(2^2 - 4^2)^2} + \frac{1}{L_6(2^2 - 6^2)^2} + \dots \right\}, & \frac{1}{L_1(2^2 - 1^2)^2}, & \frac{1}{L_1(2^2 - 1^2)^2}, & 1 & \frac{1}{L_3(2^2 - 3^2)^2}, & \dots \\ \epsilon \left\{ \frac{1}{L_1(3^2 - 1^2)^2} + \frac{1}{L_5(3^2 - 5^2)^2} + \dots \right\}, & \frac{1}{L_2(3^2 - 2^2)^2} + \frac{1}{L_4(3^2 - 4^2)^2} + \dots, & \frac{\epsilon}{L_1(3^2 - 1^2)^2}, & \frac{1}{L_2(3^2 - 2^2)^2}, & 1 & \dots \\ \dots & \dots & \dots & \dots & \dots & \dots \end{vmatrix} \quad (6.03)$$

where ϵ is written for $\frac{3d}{2R_1}$.

Determination of Roots of $\Delta_3 = 0$.

To determine the roots of the equation $\Delta_3 = 0$ it is necessary to assume a value for θ and a value for P, and to calculate the values of the determinant formed by taking the first 1, 2, 3, 4, ..., rows and columns of Δ_3 . Owing to the fact that all the diagonal terms after the first two are equal to 1 the actual numerical value of the determinant converges to a definite limit. Taking a value of θ and a series of suitable values of P, the value of P for which Δ_3 changes sign is found by interpolation. This is the root of $\Delta_3 = 0$ which corresponds with the particular value of θ chosen. By taking a series of suitable values of θ the maximum root of $\Delta_3 = 0$ is found, and also the corresponding value of θ .

In evaluating Δ_3 for any value of P and θ the method adopted was first to find the numerical values of the terms, then to eliminate successively the third, fourth, fifth, etc., rows and columns. The effect of this procedure was to alter the values of the first four terms in the top left-hand corner of Δ_3 . It was found, however, that after this operation had been repeated a few times no further alteration occurred, the effect of the distant terms being too small to be appreciated. By treating the determinant in this way it became obvious how many rows and columns should be taken in order to evaluate the root to the order of approximation which was desired.

Evaluation of P and θ for the case when μ lies between 0 and 1.

The case first solved was that for which d is negligible compared with R_1 —that is to say, the space between the cylinders is very small compared with their radii. Taking $\mu = 0$ and $\theta = 1$ it was found that if the first term only of Δ_3 is taken, the root is $P = 0.0571$. This result has already been given (*see* p. 311). On taking four rows and columns the root is $P = 0.0577$, an increase of 1 per cent. On taking six rows and columns the further change in the root is of order 0.1 per cent. It appears, therefore, that if an accuracy of 1 per cent. is desired it is unnecessary to take more than four rows and columns of Δ_3 . Moreover, it was found that practically the whole change from 0.0571 to 0.0577 is due to the terms involving the factor $(2^2 - 1^2)^{-2}$.

Under these circumstances it appeared probable that the root of $\Delta_3 = 0$ could be obtained by adding a small correction of about 1 per cent. to the highest root of $f_1 = 0$, where f_1 is written for the first term of Δ_3 , namely,

$$f_1 = \frac{1^2 + \theta^2}{L_1} + \frac{3^2 + \theta^2}{L_3} + \dots$$

It has already been pointed out that as $\mu \rightarrow 1$ the root of $\Delta_3 = 0$ approaches that of $f_1 = 0$. It is clear that for all values of μ between 0 and 1 a small correction to the root of $f_1 = 0$ can be found which will give the root of $\Delta_3 = 0$.

The value of this correction which will be called $\delta_1 P$ may be found as follows: Taking four rows and columns of Δ_3 the part of Δ_3 due the extra terms containing $(2^2 - 1^2)^{-2}$ is found to be

$$-\frac{\left(f_1 - \frac{1^2 + \theta^2}{L_1}\right)\left(f_2 - \frac{2^2 + \theta^2}{L_2}\right)}{(2^2 - 1^2)^4 L_1 L_2},$$

where f_2 is the second diagonal term in Δ_3 , namely,

$$\frac{2^2 + \theta^2}{L_2} + \frac{4^2 + \theta^2}{L_4} + \dots$$

If P_1 is the root of $f_1 = 0$, $P_1 + \delta_1 P$ is the root of $\Delta_3 = 0$, if

$$\frac{\partial \Delta_3}{\partial P} \delta_1 P - \frac{\left(f_1 - \frac{1^2 + \theta^2}{L_1}\right)\left(f_2 - \frac{2^2 + \theta^2}{L_2}\right)}{L_1 L_2 (2^2 - 1^2)^4} = 0. \quad (7.00)$$

The approximate value of Δ_3 is $f_1 f_2$ so that

$$\frac{\partial \Delta_3}{\partial P} = f_1 \frac{\partial f_2}{\partial P} + f_2 \frac{\partial f_1}{\partial P}, \quad (7.01)$$

and since $f_1 = 0$,

$$\frac{\partial \Delta_3}{\partial P} = f_2 \frac{\partial f_1}{\partial P}. \quad (7.02)$$

Differentiating f_1 it is found that

$$\frac{\partial f_1}{\partial P} = -\left(\frac{1^2 + \theta^2}{L_1^2} \frac{\partial L_1}{\partial P} + \frac{3^2 + \theta^2}{L_3^2} \frac{\partial L_3}{\partial P} + \dots\right). \quad (7.03)$$

And, since in this case $L_m = \frac{\pi^2}{16m^2} \left(\frac{1 + \mu}{1 - \mu} - \frac{P}{\theta^2} (\mu^2 + \theta^2)^3\right)$,

$$\frac{\partial L_m}{\partial P} = -\frac{\pi^2 (m^2 + \theta^2)^3}{16m^2 \theta^2}. \quad (7.04)$$

Hence

$$\frac{\partial f_1}{\partial P} = \frac{\pi^2}{16\theta^2} \sum_{m \text{ odd}} \frac{(m^2 + \theta^2)^4}{m^2 L_m^2}. \quad (7.05)$$

Hence combining (7.00) and (7.05)

$$\delta_1 P = \frac{\left(f_1 - \frac{1^2 + \theta^2}{L_1}\right)\left(f_2 - \frac{2^2 + \theta^2}{L_2}\right)}{(2^2 - 1^2)^4 L_1 L_2 f_2} \frac{\pi^2}{16\theta^2} \sum_{m \text{ odd}} \frac{(m^2 + \theta^2)^4}{m^2 L_m^2}. \quad (7.06)$$

In this expression $f_1 - \frac{1^2 + \theta^2}{L_1}$, $f_2 - \frac{2^2 + \theta^2}{L_2}$, L_2 and f_2 are negative while L_1 is positive. Hence $\delta_1 P$ is positive.

Greatest root of $f_1 = 0$.

The root, P' , of the equation

$$\sum_{m \text{ odd}} \frac{m^2 + \theta^2}{m^2 \{1 - P' (m^2 + \theta^2)^3 / \theta^2\}} = 0 \dots \dots \dots (7.07)$$

has already been evaluated for a certain range of value of θ .

It is evident that the root of

$$\sum \frac{m^2 + \theta^2}{m^2 \left\{ \frac{1 + \mu}{1 - \mu} - P' (m^2 + \theta^2)^3 / \theta^2 \right\}} = 0$$

is $P = \left(\frac{1 + \mu}{1 - \mu} \right) P'$.

In the case when $\theta = 1$, the root of $f_1 = 0$ is, therefore,

$$P = 0.0571 \left(\frac{1 + \mu}{1 - \mu} \right) \dots \dots \dots (7.08)$$

Evaluation of Correction to Root of $f_1 = 0$ and to θ .

Using this value (7.08) in evaluating the various constituents of (7.06) it is found that

$$\delta_1 P = 0.00056 \left(\frac{1 - \mu}{1 + \mu} \right) \dots \dots \dots (7.09)$$

This correction tends to zero when $\mu \rightarrow 1$ as was to be expected.

The next step is to find out whether this correction varies sufficiently with θ to alter the value of P which corresponds with the maximum root of $\Delta_3 = 0$. On inserting the values $\theta^2 = 1.2$ and $\theta^2 = 0.8$ in (7.06) it was found that $\delta_1 P$ increases with increasing values of θ , but that the increase is not sufficient to alter materially the maximum value of P . It is found that there is a slight increase in the value of θ which corresponds with the maximum value of P , but in the range of μ from 0 to 1 it is too slight to be worth discussing.

For the case when d is negligible compared with R_1 the greatest root of Δ_3 , therefore, occurs when $\theta = 1$ and it is

$$P = 0.0571 \left(\frac{1 + \mu}{1 - \mu} \right) + 0.00056 \left(\frac{1 - \mu}{1 + \mu} \right) \dots \dots \dots (7.10)$$

Root of $\Delta_3 = 0$ when d/R_1 is small, but is not neglected.

Returning now to the expression (6.03) for Δ_3 , it will be seen that the ratio d/R_1 occurs in every term, either in the factor ϵ or in L_m . The terms containing ϵ are small compared with the terms which give rise to the terms $0.00056 \left(\frac{1-\mu}{1+\mu} \right)$ in (7.10) and as we are only considering at present the range of value of μ for which this is small compared with $0.0571 \left(\frac{1+\mu}{1-\mu} \right)$, it follows that all the terms in ϵ can be neglected. The correction to the expression (7.10) due to the fact that d/R_1 is not indefinitely small therefore appears in the analysis only as a change in the values of the terms L_m ; and in these terms it always appears as a correction to be subtracted from the factor $\frac{1+\mu}{1-\mu}$. This correction may be divided into two parts.

(a) The part $d/2R_1$ which is the same for all values of m , and (b) the part $\frac{3d}{2m^2\pi^2}$ which becomes very small when m is large, but amounts to $\frac{1}{4}$ of $d/2R_1$ for $m = 1$. If the second part (b) did not exist, then evidently the approximate root of $\Delta_3 = 0$ given by (7.10) would still apply if $\frac{1+\mu}{1-\mu} - \frac{d}{2R_1}$ were substituted for $\frac{1+\mu}{1-\mu}$.

On looking at the expression (5.42) it will be noticed that owing to the factor $(m^2 + \theta^2)^3$ which occurs associated with P in the expression for L_m , the part contributed by the whole of the factor $\frac{1+\mu}{1-\mu} - \frac{d}{R_1} \left(\frac{1}{2} + \frac{3}{2m^2\pi^2} \right)$ becomes very small compared with $(\theta^2 + m^2)^3 P/\theta^2$ as m increases. Hence it appears that if the part (b) were taken as constant and equal to $\frac{3d}{2\pi^2 R_1}$ for all values of m , very little error would be caused. To estimate its magnitude, the errors in L_1, L_2, L_3 and L_4 due to this erroneous approximation have been calculated for the most unfavourable case which will be required, namely, $P = 0.05$, $\theta = 1$, $\mu = 0$, $d/R_1 = \frac{1}{3}$. The errors are: in L_1 , 0; in L_2 , 0.7 per cent.; in L_3 , 0.1 per cent.; in L_4 , 0.02 per cent. The errors in $L_1 L_2 \dots$ are therefore never so great as 1 per cent. if this approximation is used.

The object with which these approximate calculations were undertaken was to provide a basis for comparison with experiments. As measurements of the speed at which instability sets in can hardly be expected to attain an accuracy greater than 1 per cent. it does not seem worth while to attempt to attain greater precision than this. We shall therefore substitute $\left(\frac{1}{2} + \frac{3}{2\pi^2} \right) \frac{d}{R_1}$ or $0.652 \frac{d}{R_1}$ for $\left(\frac{1}{2} + \frac{3}{2\pi^2 m^2} \right) \frac{d}{R_1}$ in (5.42).

The value of P is therefore to this order of approximation given by the expression

$$P = 0.0571 \left(\frac{1+\mu}{1-\mu} - 0.652 \frac{d}{R_1} \right) + 0.00056 \left(\frac{1+\mu}{1-\mu} - 0.652 \frac{d}{R_1} \right)^{-1}. \quad (7.11)$$

This, together with the definition of P , (5.43), forms the criterion for stability. The expression (7.11) may be expected to hold for positive values of μ from 0 to 1, but it holds over a greater range than this. It holds in fact till the second term ceases to be a small correction. In calculating numerical values for P it was found that this occurred, in the cases considered, at about the value $\mu = -0.5$.

Evaluation of the Root of $\Delta_3 = 0$ when μ is Negative.

In the case when μ is negative, that is when the cylinders rotate in opposite directions it is necessary to take account of several rows and columns of Δ_3 . Being unable to discover any approximate formula of the type given in (7.11), it was decided to select particular values for μ , R_1 and R_2 , substitute in equation (6.03), and determine the maximum value of P and the corresponding value of θ by arithmetical exploration. It was expected that the results so obtained would bear a qualitative resemblance to the results obtained with any other negative value of μ .

The particular values chosen were $\mu = -1.5$, $R_1 = 3.80$ c.m., $R_2 = 4.035$ c.m. These values were chosen because, at the time this part of the work was begun, some of the measurements to be described in the second part of this paper had already been carried out by means of an apparatus which consisted of two cylinders of these two radii.

A certain amount of preliminary exploration was first undertaken. Assuming the value $\theta = 1$ the values of the determinants formed by taking the first 1, 2, 3, 4, ... etc., rows and columns of Δ_3 were found. Calling these Δ_{11} , Δ_{22} , Δ_{33} , ... it was found that they formed a series which appeared to converge rapidly to a definite limit after the fourth or fifth terms; it was found also that the limit towards which the series appeared to converge changed sign as P passed through a value in the neighbourhood of 0.001.

Further exploration seemed to show that the root increased as θ increased; accordingly after a number of trials to determine more precisely the range within which the root lay, the values of Δ_{11} , Δ_{22} , ..., Δ_{88} were calculated for values of P which appeared to lie on opposite sides of the root. These calculations were performed for the following values of θ^2 , 1.5, 2.0, 2.25, 3.0, 4.0, 5.0. In this way the table (II) was constructed. In this table the values of θ and θ^2 are given in the first two columns. The third column contains assumed values of P . The fourth to the eighth columns contain the values of Δ_{44} , Δ_{55} , Δ_{66} , Δ_{77} and Δ_{88} . The last column contains the value of P obtained by assuming that Δ_{88} varies uniformly with P in the small range between the two calculated values on either side of the root.

On inspecting the table it will be seen that the convergence of the determinant is very rapid after the fourth row and column, and that very little advantage is gained by using eight rows and columns instead of six or seven. On the other hand it was necessary to carry the calculations as far as Δ_{88} in order to be certain that this was the case.

TABLE II.—Values of Determinants used in calculating Roots of $\Delta_3 = 0$ when $\mu = -1.5$.

θ .	θ^2 .	P.	$\Delta_{44} \times 10^{-4}$.	$\Delta_{55} \times 10^{-4}$.	$\Delta_{66} \times 10^{-4}$.	$\Delta_{77} \times 10^{-4}$.	$\Delta_{88} \times 10^{-4}$.	Calculated Root.
1.225	1.5	0.0012	-0.55	-1.33	-0.86	—	—	0.00124
		0.0013	+1.08	+0.66	+1.06	—	—	
1.414	2.0	0.0012	-0.08	-2.12	-1.30	-1.19	-1.18	0.001286
		0.0013	+0.88	-0.58	+0.10	+0.17	+0.20	
1.50	2.25	0.0013	+0.96	-1.07	-0.19	-0.14	-0.13	0.00131
		0.0014	+2.07	+0.57	+1.03	+1.19	+1.22	
1.73	3.0	0.0013	+2.38	-2.36	-1.06	-0.90	-0.86	0.00134
		0.0014	+3.50	+0.09	+1.09	+1.23	+1.26	
2.0	4.0	0.0012	+4.61	-7.30	-6.18	-4.57	-4.63	0.00130
		0.0013	+6.81	-0.67	-0.35	-0.12	-0.07	
		0.0014	+4.40	+2.48	+3.37	—	—	
2.236	5.0	0.0012	+13.91	-3.61	-0.83	-0.41	-0.31	0.00121
		0.0013	+16.1	+2.8	+4.8	+5.2	+5.3	
		0.0014	+16.9	+6.5	+8.3	+8.4	+8.5	
		0.0015	+17.5	+9.65	+10.9	+11.0	+11.1	

To find the maximum value of P the roots given in the last column of Table II. were plotted on a diagram, the ordinates being the corresponding values of θ . This diagram is shown in fig. 3. It will be seen that a smooth curve can be drawn through all the

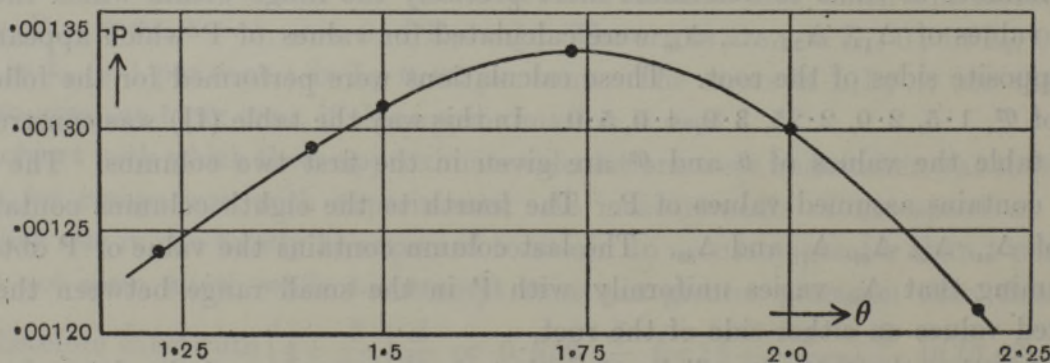


Fig. 3.

points, and that the maximum height of this curve occurs when $\theta = 1.73$, and that at this point

$$P = 0.00134. (7.13)$$

In calculating the determinants given in Table II it was found that the effect of the correction due to all the terms containing ϵ in Δ_3 was small compared with the correction $0.652 d/R_1$ which is subtracted from $\frac{1+\mu}{1-\mu}$. If the effect of the terms containing ϵ be neglected, the work just described is applicable to other values of d and R_1 , but the value of μ must be altered so that the value of $\frac{1+\mu}{1-\mu} - 0.652 \frac{d}{R_1}$ is the same as it was in the case which has been calculated.

In this way, for instance, in the case when $R_1 = 3.55$, $R_2 = 4.035$ it is found that the values $\theta = 1.73$, $P = 0.00134$ apply when

$$\mu = -1.347. \dots \dots \dots (7.14)$$

Stream Lines when Instability sets in.

The results which were obtained in the preceding section will be used later in comparing the actual disturbances which arise in unstable fluid flow with those predicted theoretically. In the meantime it is of interest to construct some diagrams showing the stream lines which are to be expected when instability sets in. These diagrams are useful in designing apparatus for testing the mathematical predictions, because the selections of the most suitable experimental method for demonstrating the instability of the flow, if it exists, will depend on the particular type of instability which is expected.

The particles of water flow in complicated three-dimensional curves. On the other hand the component of velocity in any meridian plane through the axis can evidently be represented by the Stokes Stream Function ψ . In the general case ψ is related to u by the relation $u = \frac{1}{r} \frac{\partial \psi}{\partial r}$, so that

$$\psi = \frac{r}{\lambda} e^{\sigma t} \cos(\lambda z) \sum_{m=1}^{\infty} \alpha_m B_1(\kappa_m r). \dots \dots \dots (7.20)$$

Dropping the factor $e^{\sigma t}/\lambda$ which does not affect the forms of the stream lines, in the approximate case when the asymptotic expression (5.21) is used for $B_1(\kappa_m r)$, this becomes

$$\psi = (R_1 + y)^{\frac{1}{2}} \cos(\theta \kappa z) \sum \alpha_m \sin m \kappa y. \dots \dots \dots (7.21)$$

To construct the stream lines it is necessary therefore to calculate the constants α_m . Two cases will be considered : (a) the case where μ is nearly equal to 1, and (b) the case where $\mu = -1.5$.

(a) *Stream Lines when $\mu = 1$, $\theta = 1$.*—In this case the values of α_m can be obtained directly from an inspection of equation (6.00). Retracing the operations by which 6.00 was derived from (5.43) and leaving out an arbitrary constant which determines the magnitude of the disturbance, it will be found that when m is odd

where

$$\left. \begin{aligned} \alpha_m &= \frac{\theta^2 + 1}{mL_m}, \\ L_m &= \frac{\pi^2}{16m^2} \{1 - 0.0571(m^2 + 1)^3\}, \\ \alpha_m &= 0. \end{aligned} \right\} \dots \dots \dots (7.22)$$

when m is even

The values of α_m obtained from (7.22) are given below (Table III).

TABLE III.

$a_1 = +0.210$	$a_5 = -0.0070$	$a_9 = -0.0013$	$a_{13} = -0.00045$
$a_3 = -0.0306$	$a_7 = -0.0028$	$a_{11} = -0.00074$	—

Using these values of α_m the values of $\sum a_m \sin m\kappa y$ were calculated for values of y ranging from 0 to d , or π/κ . These are given in Table IV, and are plotted in the curve

TABLE IV.

$18y/d$	0 and 18	0.5 and 17.5	1 and 17.	2 and 16.	3 and 15.	4 and 14.
$\sum a_m \sin m\kappa y$	0	0.0038	0.0109	0.0408	0.0733	0.1138
$18y/d$	5 and 13	6 and 12	7 and 11	8 and 10	9	—
$\sum a_m \sin m\kappa y$	0.1513	0.1855	0.2136	0.2300	0.2347	—

of fig. 4. It will be seen that the curve touches the axis at $y = 0$ and $y = d$, as was to be expected.

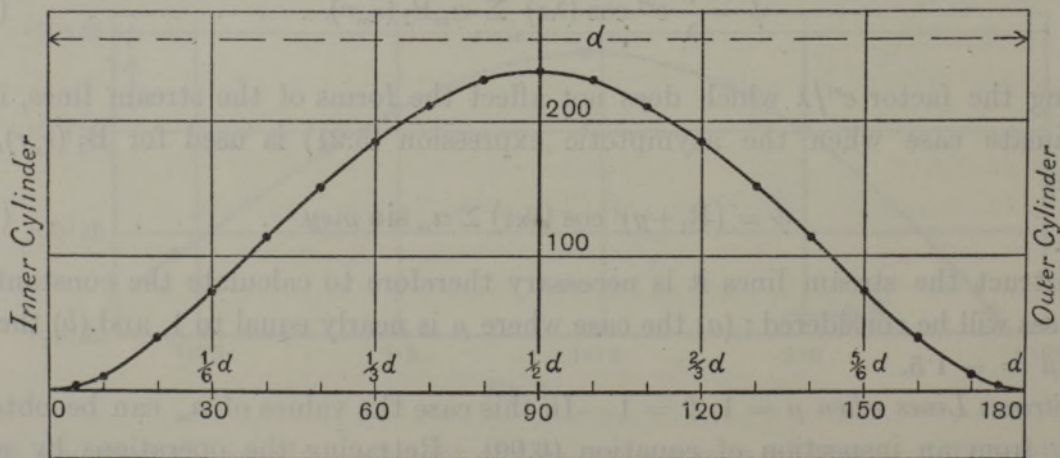


Fig. 4. Radial velocity u_1 on an arbitrary scale. Case when cylinders rotate in same direction, μ positive. Figures on under side of base line are values of $\pi y/d$ in degrees.

The value of ψ was next calculated for the case when d is small compared with R_1 , so that the factor $\sqrt{R_1+y}$ in (7.21) can be regarded as a constant. Curves were then drawn for various equidistant values of ψ , the numbers given in Table IV being multiplied by a factor so as to make $\psi = \pm 1$ at the centres of the pattern and $\psi = 0$ at

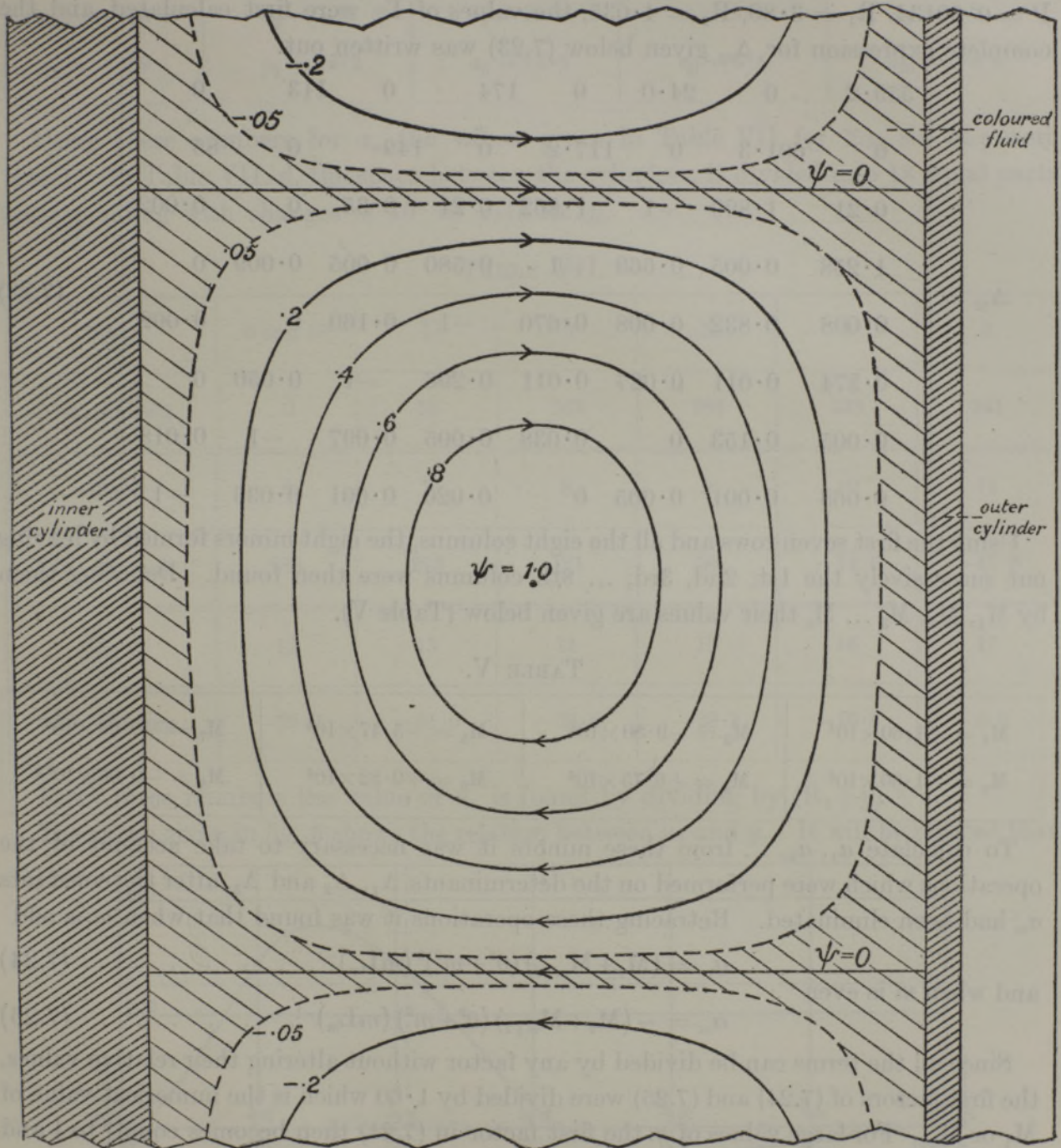


Fig. 5. Stream lines of motion after instability has set in, μ positive.

the boundary. These curves are shown in fig. 5. Their spacing gives an idea of the velocity of the flow at any point. It will be seen that the circulation in a section of the fluid by an axial plane consists of a series of vortices which fill square compartments

extending from the inner to the outer cylinder. Alternate vortices rotate in opposite directions as though they were geared together.

(b) *Stream Lines when $\mu = -1.5, \theta = 1.73$.*—In the case when $\mu = -1.5$ it was necessary first to calculate the minors of Δ_3 . Using the values $\mu = -1.5, \theta = 1.73, P = 0.00134, R_1 = 3.80, R_2 = 4.035$, the values of L_m were first calculated, and the complete expression for Δ_{ss} given below (7.23) was written out.

$$\Delta_{ss} = \begin{vmatrix} 559.2 & 0 & 24.0 & 0 & 174 & 0 & 113 & 0 \\ 0 & 601.3 & 0 & 117.2 & 0 & 149 & 0 & 85 \\ 0.21 & 1.899 & -1 & 1.862 & 0.21 & 0.35 & 0 & 0.002 \\ 1.258 & 0.005 & 0.669 & -1 & 0.580 & 0.005 & 0.009 & 0 \\ 0.008 & 0.832 & 0.008 & 0.670 & -1 & 0.160 & 0 & 0.002 \\ 0.374 & 0.011 & 0.027 & 0.011 & 0.296 & -1 & 0.050 & 0 \\ 0.005 & 0.153 & 0 & 0.038 & 0.005 & 0.097 & -1 & 0.018 \\ 0.065 & 0.001 & 0.005 & 0 & 0.020 & 0.001 & 0.033 & -1 \end{vmatrix} \quad (7.23)$$

Using the first seven rows and all the eight columns, the eight minors formed by leaving out successively the 1st, 2nd, 3rd, ... 8th columns were then found. Denoting them by $M_1, M_2, M_3 \dots M_8$ their values are given below (Table V).

TABLE V.

$M_1 = +1.60 \times 10^4$	$M_3 = -9.80 \times 10^4$	$M_5 = -3.47 \times 10^4$	$M_7 = -0.09 \times 10^4$
$M_2 = -1.60 \times 10^4$	$M_4 = +6.75 \times 10^4$	$M_6 = +0.82 \times 10^4$	$M_8 = -0.06 \times 10^4^*$

To calculate a_1, a_2, \dots from these minors it was necessary to take account of the operations which were performed on the determinants Δ_1, Δ_2 and Δ_3 , after the constants a_m had been eliminated. Retracing these operations it was found that when m is odd

$$a_m = (M_1 + M_{m+2}) (\theta^2 + m^2)^2 (mL_m)^{-1}, \dots \dots \dots (7.24)$$

and when m is even

$$a_m = -(M_2 + M_{m+2}) (\theta^2 + m^2) (mL_m)^{-1}. \dots \dots \dots (7.25)$$

Since all the terms can be divided by any factor without altering their relative values, the first factors of (7.24) and (7.25) were divided by 1.60 which is the numerical value of M_1 or M_2 . For large values of m the first factor in (7.24) then becomes equal† to 1 and

$$a_m = (\theta^2 + m^2) (mL_m)^{-1}. \dots \dots \dots (7.26)$$

* M_8 is probably slightly inaccurate owing to the method of reduction, but as will be seen later such an inaccuracy would have no appreciable effect on the result.

† The part due to M_{m+2} is small compared with the part due to M_1 , so that errors in a_m due to errors in M_{m+2} become unimportant as m increases.

Using the formulæ (7.24) and (7.25) for the first six terms and (7.26) for the higher terms, the following series of values were found for a_m (see Table VI).

TABLE VI.

$a_1 = -123.5$	$a_3 = -67.8$	$a_5 = 21.6$	$a_7 = 9.4$	$a_9 = 4.6$
$a_2 = -189$	$a_4 = 18.2$	$a_6 = 13.8$	$a_8 = 6.4$	$a_{10} = 3.4$

Using these numbers for a_m the values given in Table VII for $\Sigma a_m \sin m\kappa y$ were found. In Table VII, d , the space between the cylinders, is divided into 18 equal parts corresponding with changes of 10° or $\pi/18$ in κy .

TABLE VII.

$18y/d$	0 and 18	1	2	3	4	5
$\Sigma a_m \sin m\kappa y$	0	55	164	284	348	341
$18y/d$	6	7	8	9	10	11
$\Sigma a_m \sin m\kappa y$	288	213	121	39	-14.6	-47.8
$18y/d$	12	13	14	15	16	17
$\Sigma a_m \sin m\kappa y$	-59.0	-51.0	-38.8	-28.1	-16.8	-5.0

From these numbers the value of u_1 is found by dividing by $(R_1 + y)^{-\frac{1}{2}}$.

The curve given in fig. 6 shows the relation between u_1 and y . It will be noticed that

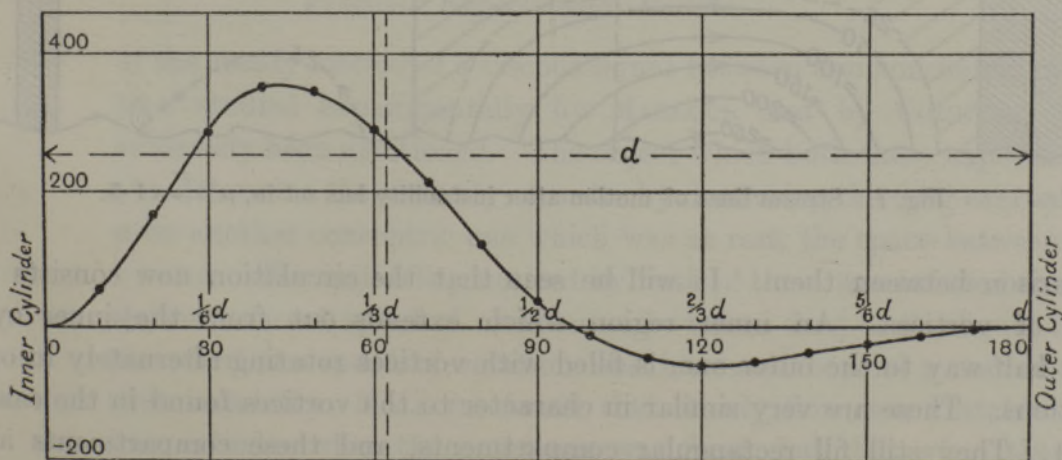


Fig. 6. Radial velocity u_1 on an arbitrary scale; case when cylinders rotate in opposite directions, $\mu = 1.5$.

as was to be expected the curve touches the axis at either end. The interesting thing about it, however, is that it crosses the axis at a point roughly half-way between the two cylinders. At this point the radial component of velocity is zero. This means that there is a certain cylindrical surface between the two rotating cylinders which divides the flow. The instability therefore produces a flow which is divided into two separate regions.

The stream lines of this flow were next calculated in the same way as in the previous case. They are shown in fig. 7, which is printed on the same scale as fig. 5 to facilitate

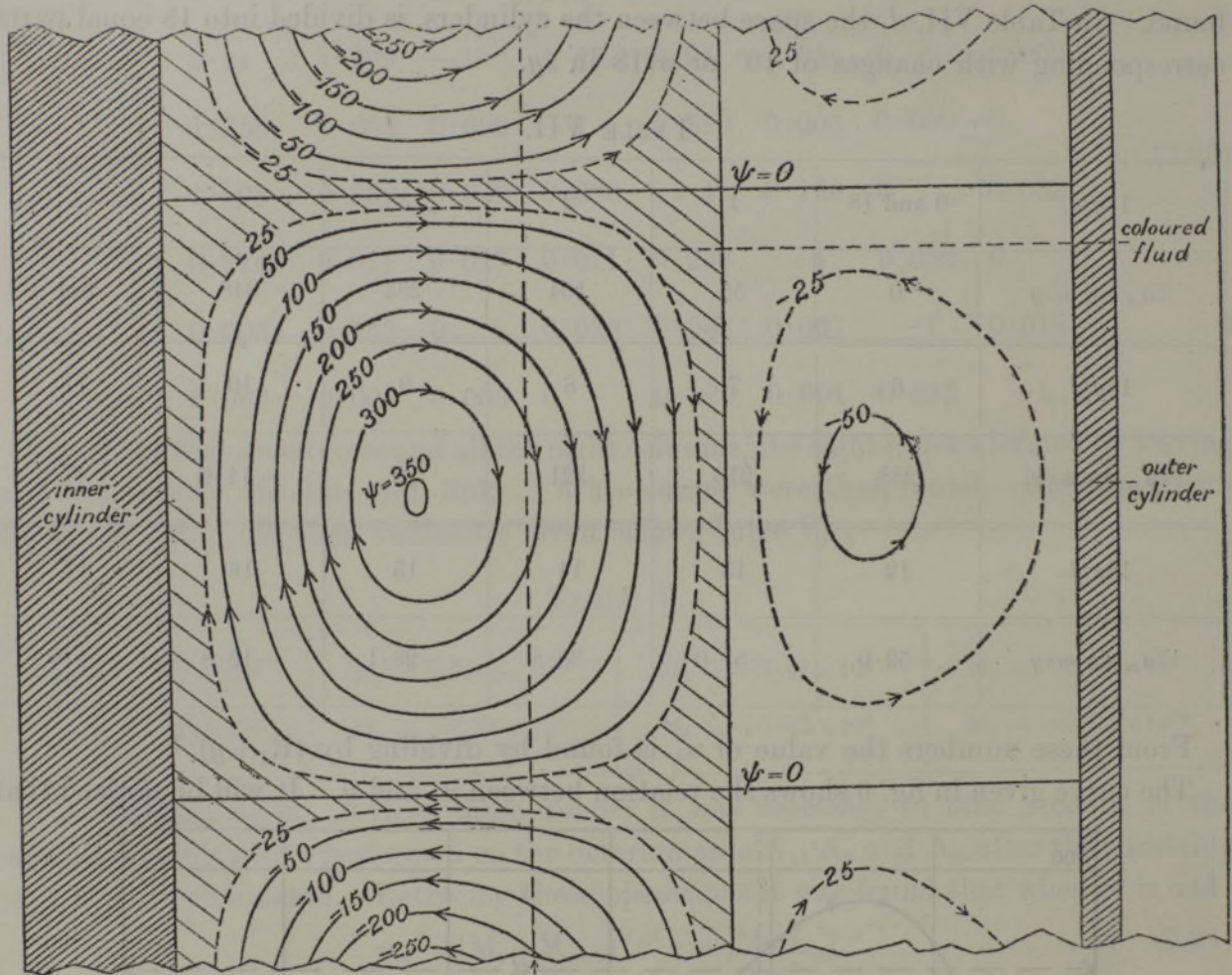


Fig. 7. Stream lines of motion after instability has set in, $\mu = -1.5$.

comparison between them. It will be seen that the circulation now consists of two types of vortices. An inner region which extends out from the inner cylinder, about half-way to the outer one, is filled with vortices rotating alternately in opposite directions. These are very similar in character to the vortices found in the case when $\mu = 1$. They still fill rectangular compartments, and these compartments are still nearly square, though not so accurately square as in the case when $\mu = 1$. An effect of restricting the inner circulation to a region which is only about half the thickness of

the total space between the cylinders appears to be to reduce also the spacing of the other sides of the rectangular boundaries of the vortices so that the compartments are still nearly square.

In the space outside the inner system of vortices is an outer system which is very much less vigorous than the inner system. These outer vortices rotate in the opposite directions to the inner ones with which they are in contact.

It seems probable that the physical explanation of this phenomenon is that the surface where the velocity is zero in the steady motion divides the space between the two cylinders into two regions. In the inner region the square of the circulation decreases outwards, so that centrifugal force tends to make the flow unstable. In the outer region the square of the circulation increases so that centrifugal force tends to make the flow stable. The surface where the fluid is at rest in the steady motion is not coincident with the surface separating the two systems of vortices in the disturbed motion. In fig. 7 the section of the former surface is shown as a dotted line, and it will be seen that the inner system of vortices extends outside the region where centrifugal force tends to produce instability. That this would be the case might have been anticipated on general grounds.

A remarkable feature of the vortex systems shown in fig. 7 is the great difference which exists between the vigour of the inner and outer systems. The stream lines are drawn for values of ψ differing by 50 units on an arbitrary scale. There are six of these in the inner system and only one in the outer system. To show up more clearly the general features of the circulations, two intermediate stream lines have been drawn for the values $\psi = +25$ and $\psi = -25$. These are dotted to differentiate them from the other stream lines. The shaded portions of the diagrams, figs. 5 and 7, will be referred to in the second part of this paper.

PART II.—EXPERIMENTAL.

Previous Experimental Results.

The stability of the steady motion of a viscous liquid between two concentric rotating cylinders has been studied experimentally by MALLOCK and by COUETTE. These experiments have already been mentioned. The object which both these experimenters had in view was to determine the viscosity of water by measuring the drag exerted by a rotating cylinder on another concentric one which was at rest, the space between them being filled with water. The instability noticed by both of them was inferred from the fact that the relation between speed of rotation and viscous drag of the liquid ceased to be a linear one when the speed of rotation was increased beyond a certain limit. Using this test for instability, MALLOCK found that steady flow was unstable at all

This figure does not agree with fig. 6. The left-hand boundary should be the outside line of the diagram on the right. Approx.
J.P. Mas 4.7.1961

the total space between the cylinders appears to be to reduce also the spacing of the other sides of the rectangular boundaries of the vortices so that the compartments are still nearly square.

In the space outside the inner system of vortices is an outer system which is very much less vigorous than the inner system. These outer vortices rotate in the opposite directions to the inner ones with which they are in contact.

It seems probable that the physical explanation of this phenomenon is that the surface where the velocity is zero in the steady motion divides the space between the two cylinders into two regions. In the inner region the square of the circulation decreases outwards, so that centrifugal force tends to make the flow unstable. In the outer region the square of the circulation increases so that centrifugal force tends to make the flow stable. The surface where the fluid is at rest in the steady motion is not coincident with the surface separating the two systems of vortices in the disturbed motion. In fig. 7 the section of the former surface is shown as a dotted line, and it will be seen that the inner system of vortices extends outside the region where centrifugal force tends to produce instability. That this would be the case might have been anticipated on general grounds.

A remarkable feature of the vortex systems shown in fig. 7 is the great difference which exists between the vigour of the inner and outer systems. The stream lines are drawn for values of ψ differing by 50 units on an arbitrary scale. There are six of these in the inner system and only one in the outer system. To show up more clearly the general features of the circulations, two intermediate stream lines have been drawn for the values $\psi = +25$ and $\psi = -25$. These are dotted to differentiate them from the other stream lines. The shaded portions of the diagrams, figs. 5 and 7, will be referred to in the second part of this paper.

PART II.—EXPERIMENTAL.

Previous Experimental Results.

The stability of the steady motion of a viscous liquid between two concentric rotating cylinders has been studied experimentally by MALLOCK and by COUETTE. These experiments have already been mentioned. The object which both these experimenters had in view was to determine the viscosity of water by measuring the drag exerted by a rotating cylinder on another concentric one which was at rest, the space between them being filled with water. The instability noticed by both of them was inferred from the fact that the relation between speed of rotation and viscous drag of the liquid ceased to be a linear one when the speed of rotation was increased beyond a certain limit. Using this test for instability, MALLOCK found that steady flow was unstable at all speeds of the inner cylinder when the outer one was fixed, but that when the outer cylinder was rotated the flow was stable for low speeds, unstable for high speeds, and sometimes stable and sometimes unstable over a range of intermediate speeds.

No indication of the existence of any sharp or definite criterion for stability was observed.

These results disagree entirely with the theoretical predictions made in the first part of this paper. According to the foregoing theory the motion should be stable even at high speeds when the inner cylinder is at rest. When the outer cylinder is at rest the flow should be stable at low speeds of the inner cylinder, and there should be a definite speed at which instability should suddenly make its appearance as the speed is increased.

This disagreement between theory and experiment may be due to a variety of causes. It may be that the types of disturbance which actually arise are not symmetrical about the axis. On the other hand there are other possible causes besides instability which could give rise to a non-linear relation between speed of rotation and viscous drag in MALLOCK'S experiments. In the first place the lengths of MALLOCK'S cylinders were very little greater than their diameters. His outer cylinder for instance was 7·8 inches diameter while the depth of water used was only 8·5 inches, and the thickness of the layer of water between the cylinders was 0·915 and 0·42 inches, in his two sets of experiments. If the cylinders were infinitely long or if the thickness of the layer of fluid were very small, the steady two dimensional flow contemplated in MALLOCK'S experiments would no doubt occur, and a linear relation might be expected between speed and viscous drag. On the other hand in the neighbourhood of the bottom of the liquid the flow cannot be two-dimensional, and unfortunately the cylinder on which MALLOCK measured the viscous drag extended practically down to the bottom of the liquid. It therefore certainly penetrated into the region where the linear law does not hold. MALLOCK recognised this, for in the course of his experiments he substituted an ingenious mercury bottom for the rigid bottom with which he began. By this means he hoped to eliminate, partially at any rate, the effect of the bottom. The very large effect which this device had on his results showed that in his original experiments, at any rate, a large part of the drag which he observed might be attributed directly to the effect of the bottom. On the other hand, there is little evidence to show that it succeeded in eliminating this effect completely, or even that the bottom effect was not still large in the case when the outer cylinder was at rest.

It appears therefore that MALLOCK'S experiments do not afford conclusive evidence of the existence of instability in the case when the outer cylinder is at rest, at any rate at slow speeds of the inner cylinder.

In the case when the inner cylinder is at rest MALLOCK'S experiments appear more conclusive, because he observed sudden and violent changes in the drag on the inner cylinder. On the other hand it is by no means certain that this instability would have occurred if the inner cylinder had been supported differently. It has been shown by VON HOPF that instability may arise from flexibility in the bounding walls of a fluid in steady motion. In MALLOCK'S experiments one of the cylinders had to be supported so that it could turn without resistance. This condition must, I think, have prevented this cylinder from being held so rigidly that small lateral movements were impossible.

Design of Apparatus.

In designing apparatus for testing the conclusions reached in the first part of this paper, care was taken to eliminate as far as possible the disadvantages from which, in the author's opinion, MALLOCK'S apparatus suffered. In the first place the cylinders were made as long as possible so as to eliminate end effects. They were 90 cm. long and the outer one was 4.035 cm. radius. In most of the experiments the thickness of the layer of liquid between the cylinders was less than 1 cm. In the second place both

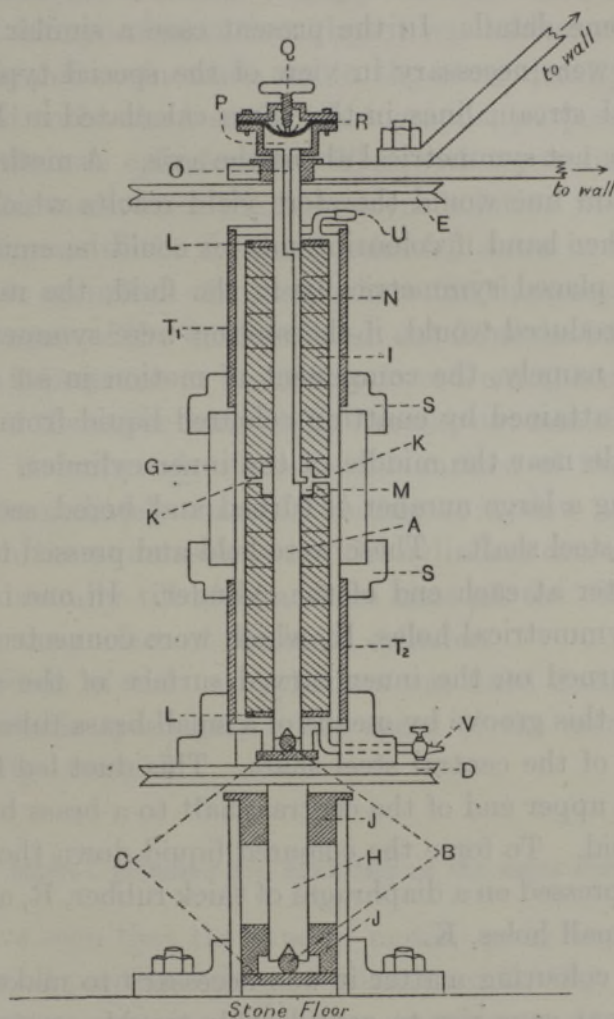


Fig. 8.

cylinders were held in heavy plane bearings at each end by heavy iron supports fixed to a stone floor and to the walls of the Cavendish Laboratory.

The general arrangement of the cylinders is shown in fig. 8. In that diagram the various parts of the apparatus are indicated by letters. The weight of each cylinder was taken by a steel ball, B, resting on a flat plate, C, below, and fitting into a conical centre in the end of the shaft which it supported. The bearings, J, were long and of exceptionally good fit, so that lateral motion could only occur by bending of the whole

apparatus. In order that this might be minimised as far as possible the inner cylinder was fixed on a mild-steel shaft, A, of large diameter ($\frac{3}{4}$ inch).

It is clear for the reasons given above that the methods of previous observers would not give the information required. It was necessary to devise some method which would show not only the exact speed at which instability occurs, but the type of motion which ensues.

The method employed by OSBORNE REYNOLDS in the case of flow through a circular pipe was to inject a thin continuous stream of colouring matter into the centre of the stream. When the breakdown of steady flow occurred the motion of the water could then be studied in some detail. In the present case a similar method was used, but certain modifications were necessary in view of the special type of motion which was expected. The actual stream lines in the cases calculated in Part I. are complicated spiral curves which are not symmetrical about the axis. A method designed to show up or mark a single stream line would therefore yield results which would be difficult to interpret. On the other hand if colouring matter could be emitted simultaneously at all points of a circle placed symmetrically in the fluid, the motion of the sheets of colouring matter so produced would, if the motion were symmetrical, give exactly the information required, namely, the component of motion in an axial plane.

This condition was attained by emitting coloured liquid from six small holes placed on a symmetrical circle near the middle of the inner cylinder. The inner cylinder, I, was made by threading a large number of turned and bored sections made of paraffin wax on to the central steel shaft. These were held and pressed together by brass discs, L, of the same diameter at each end of the cylinder. In one of the paraffin sections were six very small symmetrical holes, K, which were connected together by means of a small groove, M, turned on the inner curved surface of the section. The coloured liquid was supplied to this groove by means of a small brass tube, N, which was let into a slot cut in one side of the central steel shaft. This duct led finally through a small central hole, O, in the upper end of the central shaft to a brass box, P, which was filled with the coloured liquid. To force the coloured liquid down the duct the milled head, Q, was turned. This pressed on a diaphragm of thick rubber, R, and so forced the colour out through the six small holes, K.

In order to see the colouring matter it was necessary to make the outer cylinder of glass. This requirement gave rise to considerable trouble on account of the difficulty of producing an accurately turned, bored, ground and polished glass tube 90 cm. long. The difficulty was surmounted by Messrs. Powell, of the Whitefriars Glass Works, who succeeded in producing a satisfactory glass tube 8 inches long, 8.07 cm. bore and 10.5 cm. external diameter. This was turned, bored, roughly polished, and the ends faced square. It was then mounted in iron castings, S, which were fitted accurately on to the upper and lower sections, T₁ and T₂, of the outer rotating cylinder. These castings will be seen at the top and bottom of the photographs, figs. 9-16, Plates 4 and 5. The inside bore of the outer cylinder did not vary by as much as $\frac{1}{16}$ mm. in its whole length.

The whole apparatus was driven by an electric motor fitted with a governor so that the speed could be kept constant. The ratio of the speeds of the cylinders could be varied by means of a continuously variable speed gear.

Method of performing Experiments.

In performing an experiment the box, P, was filled with a solution of fluoresceine, which was usually made of the same density as water by mixing with ammonia or alcohol, though in some experiments it was made slightly heavier. This fluorescent solution was found to be very good for eye observations, but it was useless when photographs were to be taken. A solution of eosin made up to the same density as water by mixture with alcohol was found to be the best for photographic purposes.

The space between the two cylinders was filled with water from which air had been expelled by boiling. In cases when the fluoresceine solution was slightly heavier than water the liquid coming out of the six small holes fell down in six streams which kept fairly close to the inner cylinder. In cases where the fluoresceine solution was of the same density as water some of the water was run out from the bottom of the apparatus, and at the same time fluoresceine or eosin was forced out through the six holes. The downward movement of the water drew the fluoresceine out into six thin vertical streams, which were found to be extremely close to the surface of the inner cylinder. The apparatus was then immediately started rotating at a slow speed and the shearing motion of the liquid in the annulus between the cylinders caused the six vertical lines of colour to broaden laterally till after a short time all the coloured liquid formed a uniform thin sheet on the surface of the inner cylinder.

The ratio of the speeds of the two cylinders was fixed during each experiment by the setting of the variable speed gear. The speed of the motor was then gradually increased till instability occurred.

Case when Cylinders are Rotating in the same direction.

In this case we have seen that the type of motion to be expected when instability sets in is the same for all positive values of μ less than R_1^2/R_2^2 . The flow in meridian planes consists of vortices contained in square partitions and rotating alternately in opposite directions. The effect which this system of vortices might be expected to have on the film of coloured fluid close to the inner cylinder can be seen by referring to fig. 5, Part I. Since the motion is evidently to the first order of small quantities a steady motion, the coloured liquid which lies close to the surface $\psi = 0$ will remain close to that surface. The surface $\psi = 0$ consists of the square partitions within which the vortices are contained. The coloured liquid will therefore mark out the edges of these square partitions. In fig. 5 the shaded portion represents a possible form of the coloured region after instability has set in.

General Result.

On observing the apparatus from the side it was found that provided the experiment was carefully carried out, the instability made its appearance at a certain speed in every case when it was expected and in no case when it was not. This speed was quite definite, and the measurement could be repeated on different occasions with an accuracy of about 1 or 2 per cent.

The phenomenon which was observed was the same in each case. The layer of coloured liquid suddenly gathered itself into a series of equidistant films whose planes were perpendicular to the axis of rotation. These films were in each case spaced at a distance apart nearly equal to *twice* the thickness between the cylinders. The films seemed to spread out till they reached the inner surface of the outer cylinder. They then spread upwards and downwards close to that surface till they covered it with a thin film of coloured liquid. This film was almost invisible because it could not be seen edge-on. On the other hand, when the upward and downward flowing sheets met at the points half-way between the out-flowing films they formed inward-flowing films of the same type as the outward-flowing ones. The resulting appearance after the motion had been going on for about two or three seconds was that of a series of thin equi-distant planes of coloured fluid spaced at a distance equal to the thickness of the space between the cylinders. In fact, after the first few seconds the motion appeared to get to a steady state in which it was impossible to distinguish the outward-flowing films from the inward-flowing ones, though all of them were extremely sharply defined.

Photographs of the Stream Lines.

Considerable difficulty was experienced in obtaining satisfactory photographs of the phenomenon because when eosin was used instead of fluorescene a more concentrated solution was necessary; and it was found difficult to make up this solution so that its density remained the same as that of water when it was surrounded by water. It frequently happened in fact that the coloured liquid formed two columns, one going up and the other down, when strong eosin solution mixed with alcohol was used. In spite of this and other difficulties some fairly good photographs were obtained.

Fig. 9, Plate 4, shows the appearance of the films shortly after their formation. This photograph shows a motion which is not so regular as most of those observed, but it has the advantage that one can see some of the intermediate stream lines marked out by some colouring matter which had got away from the surface of the inner cylinder before the instability set in. A particularly noticeable one occurs in the third partition from the bottom on the left-hand side. The photographs were taken with an ordinary magnesium flashlight apparatus.

Verification of Predicted Spacing of the Vortices.

It will be noticed that the partitions shown in figs. 9, 10 and 11, Plate 4, appear square. This square appearance, however, is deceptive. The refraction of the glass and water

magnify the horizontal dimensions without altering the vertical dimensions of objects in the water. On the other hand, the outer edge of the pattern is cut off altogether by refraction. These two effects neutralise one another so that the general appearance of the partitions in the photographs is square.

The photograph (fig. 9, Plate 4) was taken when the radius of the inner cylinder, R_1 , was 2.93 cm.; R_2 , the radius of the outer cylinder, was the same in all cases, namely, 4.035 cm. The distance apart of the partitions as measured on the original photograph was 0.47 cm., the external diameter of the glass cylinder on the photograph was 4.7 cm. and its true diameter was 10.5 cm. The true distance apart of the partitions was, therefore, $10.5 \times 0.47 / 4.7 = 1.05$ cm. The difference between the radii of the two cylinders was $4.035 - 2.93 = 1.105$ cm. Hence we have our first numerical verification of the theory of Part I.

Predicted spacing of vortices	..	1.105	cm.	}	Error 5 per cent.
Observed	..	1.05	„		

To show the effect of change in thickness of the layer of fluid a photograph of the bands or partitions, taken when $R_1 = 3.25$ cm., is shown in fig. 10, Plate 4. On measuring this spacing on the original photograph it was found that twelve of them occupied 3.95 cm. The magnification was 0.4095. Hence

True spacing of partitions was	..	0.804	cm.	}	Error $3\frac{1}{2}$ per cent.
Predicted spacing was $4.035 - 3.25$..	0.785	„		

In order to show the accuracy with which these bars of coloured liquid space themselves when the experiments are carefully performed the photograph (fig. 11, Plate 4) is shown. The fineness of the partitions shown in this photograph approximates to the fineness which can easily be obtained with the fluorescense used for eye observations, but it is not actually quite so good.

Case when the Cylinders Rotate in Opposite Directions.

When μ is negative—that is, when the cylinders rotate in opposite directions, only one case has been worked out completely, namely, that in which $\mu = -1.5$, $R_1 = 3.80$, $R_2 = 4.035$. The characteristic differences revealed by the analysis between the motion in this case, and that in the case when μ is positive, are:—

- (a) The spacing of the vortices is reduced in the ratio 1.73 : 1. The predicted spacing of the vortices in this case is in fact $(4.035 - 3.80) / 1.73 = 0.136$ cm.; and
- (b) The vortices in contact with the inner cylinder only extend out about half-way to the outer cylinder instead of extending right across the fluid annulus.

(a) *Spacing of Vortices.*—To verify the conclusions reached in regard to the spacing of the vortices a number of measurements were taken when the radius of the inner cylinder was 3.80 cm., the values of μ ranging from +0.65 to -1.78.

The results are given in Table VIII. and they are shown in the form of a curve in fig. 12. In this curve the abscissæ represent μ and the ordinates represent the corresponding spacing of the vortices in centimetres. The predicted points, *i.e.*, theoretical

TABLE VIII.—Giving the Observed Spacing of the Vortices for various values of μ in the case when $R_1 = 3.80$ cm. and $R_2 = 4.035$, so that $d = 0.235$ cm.

μ .	Observed Spacing of Vortices.
0.65	0.241, 0.245.
0.596	0.25, 0.24, 0.238, 0.25.
0.40	0.244, 0.250, 0.244.
0	0.236, 0.235.
-0.388	0.230, 0.24, 0.236.
-0.492	0.237, 0.238, 0.235.
-0.640	0.232, 0.228.
-0.716	0.201, 0.203, 0.198.
-1.00	0.150, 0.165, 0.160, 0.157.
-1.20	0.156, 0.165.
-1.37	0.143, 0.146.
-1.78	0.09, 0.105, 0.115.

values of d/θ , are shown by means of circles and the observed points by means of dots. The curve is drawn roughly through the dots. Unfortunately, owing to an oversight, no observation was taken for the value $\mu = -1.5$, but it will be seen that the calculated point lies almost exactly on the observed curve.

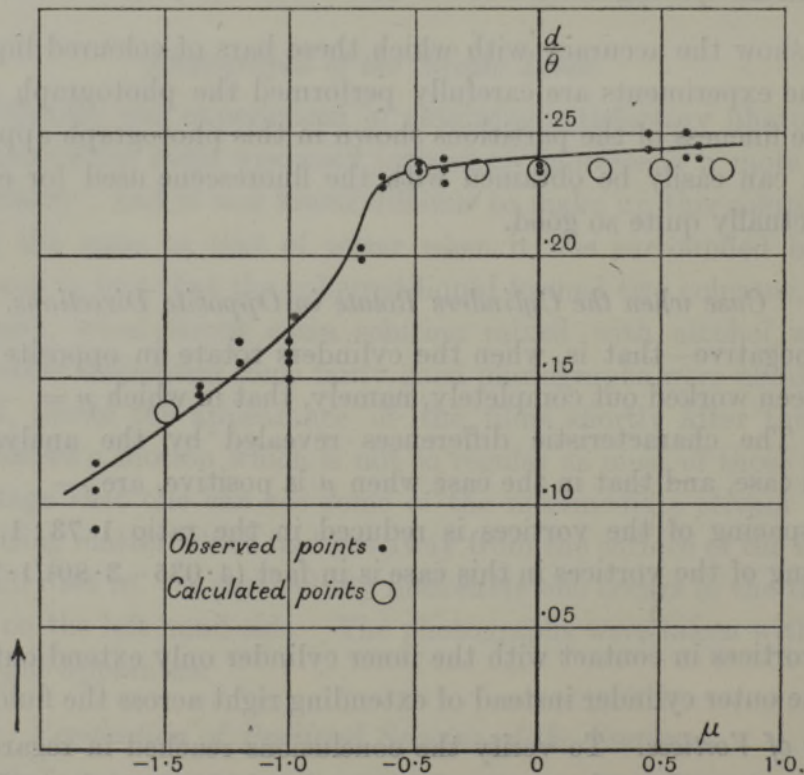


Fig. 12. Comparison between observed and predicted spacing of vortices for various values of μ ; case when $R_1 = 3.80$ cm., $R_2 = 4.035$ cm.

It will be noticed that the predicted result that the spacing of the vortices should be the same for all positive values of μ and equal to the thickness of the layer of fluid is also strikingly verified. It will be observed that the spacing of the vortices does not begin to decrease much till μ has a considerable negative value, about -0.5 .

(b) In the case when $R_1 = 3.80$ it was found difficult to verify the prediction that the vortices in contact with the inner cylinder should extend no further than about half-way out to the outer cylinder because the refraction of the glass cylinder prevented the extreme edge of this region from being seen. A simple calculation showed that this cause would make it impossible to see the outside edge of the inner circulation if it extended to within 0.37 cm. of the outer cylinder. For this reason, therefore, the inner cylinder was reduced to a diameter of 4 cm. and the photographs shown in (Plates 4 and 5) figs. 13, 14, 15 and 16 were taken. The values of μ were not measured very accurately but in figs. 13 and 14 it was about -1.05 ; in fig. 15 $\mu = -2.0$; and in fig. 16 $\mu = -2.3$.

On looking at the photographs it will be seen that the results predicted by theory are completely verified. The inner vortices do not penetrate to the outer parts of the fluid, the spacing of the vortices decreases as $-\mu$ increases, and the inner partitions remain of the same shape, approximately square, while they decrease in size with increasing values of $-\mu$.

The "spacing of the vortices" is half the wave-length—that is, half the distance apart of the centres of the ring-like figures shown in the photographs 13–16 into which the coloured liquid, initially close to the surface of the inner cylinder, suddenly forms itself when instability sets in.

Critical Speeds at which Instability appears.

Perhaps the most successful feature of the analysis contained in the first part of this paper is the accuracy with which it predicts the critical speeds at which instability appears. A number of sets of measurements were made covering a range of values of μ from $-\infty$ to $+\infty$. These will now be discussed in detail.

Case when μ is positive and > 1 or infinite, i.e., when the Outer Cylinder Rotates Faster than the Inner One and in the same Direction, or when the Inner Cylinder is at Rest.

Under these circumstances the motion was found to be completely stable even at the maximum speed of which the apparatus was capable.*

This result is in direct contradiction to that of MALLOCK, though it is in accordance with the theoretical prediction which takes account only of symmetrical disturbances. The difference might be attributed to the greater rigidity of the present apparatus, and perhaps to its greatly increased length.

* Five revolutions of the outer cylinder per second.

Critical Speeds when μ is less than R_1^2/R_2^2 .

Three complete sets of observations were taken: (1) with $R_1 = 3.00$, (2) with $R_1 = 3.80$, (3) with $R_1 = 3.55$. Each observation consisted in observing the speed of rotation of the cylinders at which the vortices appeared, *i.e.*, the speed when the partitions between the vortices suddenly spread out from the inner cylinder. In each case one or two rough readings were taken to find the approximate speed at which instability appeared. The governor was then set for this speed so that large changes in current produced only small changes in the speed. The final reading was then made by increasing the speed fairly rapidly* till the instability was on the point of occurring, then increasing the speed very gradually. In this way it was found that readings could be repeated with an average error of about 2 per cent.

When it was found that this order of accuracy could be obtained, it became clear that the temperature would have to be read with an error of 0.2° C., or less, in order that viscosity might be known accurately enough to make full use of the accuracy of the stability measurements.

The speed of one of the cylinders was measured both just before and just after the instability occurred, and the observation was rejected if it was found that too great a jump in speed had been made. With the governor employed on the motor it was found that the variations in speed with a given setting of the apparatus were less than $\frac{1}{2}$ per cent. The ratio, μ , of the speeds of the cylinders was measured by timing them over a period of two or three minutes.

In order to make the results comparable with one another it is necessary to divide the speed in each case by the coefficient of kinematical viscosity.† These coefficients were taken from KAYE and LABY'S physical tables. The results are given in Tables IX., X., and XI. In column 1 of each table is given the value of μ . In columns 2 and 3 the observed values of Ω_1/ν and Ω_2/ν , where Ω_1 and Ω_2 are the angular velocities of the inner and outer cylinders, and ν represents the coefficient of kinematical viscosity which is equal to (the coefficient of viscosity) \div (density). In column 4 in each table is given the theoretical value of Ω_1 calculated for the corresponding value of μ from the criterion given in (7.11), Part I. On comparing columns 3 and 4 it will be seen that the agreement between theory and observation is extremely good in the cases where $R_1 = 3.80$ and $R_1 = 3.55$. It is not quite so good in the case where $R_1 = 3.0$, but as the observations in this case were made before it was realised how high a degree of accuracy could be obtained in stability measurements, the temperature was only observed roughly once or twice during the experiments. Some uncertainty, therefore, exists as to the exact value of ν in this series of measurements.

* The governor did not begin to act till a certain speed had been attained.

† Two geometrically similar motions are also dynamically similar if the speed, divided by the coefficient of kinematic viscosity, is the same in the two cases.

TABLE IX.—Showing observed and calculated speeds at which instability first appears when $R_1 = 3.00$, $R_2 = 4.035$ cm.

μ .	Ω_2/ν observed.	Ω_1/ν observed.	Ω_1/ν calculated.	μ .	Ω_2/ν observed.	Ω_1/ν observed.
0.552	83.7	152.0	∞	-1.48	-130.0	87.9
0.530	51.6	97.0	105.2	-1.67	-163.0	97.0
0.520	40.1	77.2	84.9	-2.0	-236.0	118.0
0.455	28.8	63.5	50.5	-2.37	-326.0	137.0
0.423	21.6	51.1	44.5			
0.415	18.6	44.9	43.5			
0.410	19.3	47.1	42.6			
0.359	14.4	40.2	37.5			
0.245	8.6	35.3	31.6			
0	0	30.3	27.6			
-0.33	-10.6	32.1	30.0			
-0.33	-11.1	33.5	30.0			
-0.565	-21.0	37.2				
-0.60	-24.8	41.4				
-0.703	-29.8	42.3				
-0.905	-47.1	52.0				
-1.073	-67.0	62.8				
-1.285	-102.6	79.6				

TABLE X.—Observed and calculated speeds at which instability first appears when $R_1 = 3.80$, $R_2 = 4.035$ cm.

μ .	Ω_2/ν .	Ω_1/ν observed.	Ω_1/ν calculated.	μ .	Ω_2/ν .	Ω_1/ν observed.	Ω_1/ν calculated.
0.864	790.0	914.0	860.0	-0.553	-121.6	219.1	222.0
0.846	530.0	626.0	669.0	-0.621	-141.0	227.0	230.0
0.810	362.2	447.0	477.0	-1.0	-312.0	312.0	
0.788	340.0	431.5	424.0	-1.0	-320.0	320.0	
0.764	298.5	390.5	383.0	-1.0	-313.0	313.0	
0.788	278.0	353.0	424.0	-1.16	-400.7	345.3	
0.741	245.3	330.8	354.0	-1.26	-462.0	367.0	
0.666	196.3	294.0	294.0	-1.36	-539.2	396.6	
0.666	190.2	284.3	294.0	-1.428	-592.0	415.5	
0.631	172.8	273.8	276.0	-1.605	-718.0	447.5	
0.554	136.2	246.0	248.0	-1.714	-845.0	493.0	
0.450	99.1	220.1	225.0	-1.766	-876.0	496.0	
0.422	90.7	217.0	220.0	-1.916	-1005.0	524.0	
0.397	83.0	209.0	216.0	-1.953	-1056.0	540.4	
0.274	54.9	200.1	203.0	-1.996	-1104.0	553.0	
0.160	30.4	190.2	196.0	-2.24	-1362.0	608.0	
0	0	190.8	191.5	-2.51	-1672.0	666.0	
0	0	189.2	191.5	-2.865	-2113.0	737.0	
0	0	193.1	191.5	-2.891	-2120.0	733.0	
-0.082	-15.7	190.8	191.5				
-0.145	-27.8	192.0	192.3		calculated		calculated
-0.164	-31.0	189.5	193.0	-1.50	-712.0		475.0
-0.214	-41.5	192.0	194.5				
-0.378	-80.4	212.5	204.0				
-0.46	-101.5	219.0	209.0				

TABLE XI.—Observed and calculated speeds at which instability first appears when $R_1 = 3.55, R_2 = 4.035$ cm.

μ .	Ω_2/ν .	Ω_1/ν observed.	Ω_1/ν calculated.	μ .	Ω_2/ν observed.	Ω_1/ν observed.
0.765	303.0	396.0	470.0	-0.689	-66.2	96.2
0.7535	245.5	326.0	313.0	-0.793	-84.4	106.5
0.755	242.3	321.0	325.0	-0.800	-84.4	105.6
0.748	202.7	271.0	278.0	-0.843	-92.2	109.4
0.745	182.9	245.5	264.0	-1.00	-128.9	128.9
0.718	135.7	189.1	191.0	-1.00	-125.8	125.8
0.664	93.9	141.5	139.1	-1.129	-153.4	135.9
0.639	80.2	125.6	126.5	-1.244	-184.1	148.0
0.643	84.2	131.0	130.8	-1.302	-209.6	161.1
0.569	60.3	106.0	105.3	-1.489	-264.0	177.3
0.542	55.3	102.1	100.1	-1.63	-299.0	183.7
0.476	44.5	93.5	91.2	-1.795	-376.0	209.4
0.419	36.5	87.2	84.5	-1.925	-419.0	215.0
0.376	32.6	86.8	81.4	-2.00	-475.0	237.3
0.322	26.0	80.8	78.1	-2.17	-511.6	235.9
0.276	21.5	77.8	75.9	-2.32	-579.5	249.8
0.213	16.1	75.6	73.5	-2.53	-709.0	280.2
0	0	70.7	69.8	-2.68	-820.0	306.0
-0.144	-10.24	71.1	70.1	-2.84	-903.5	318.0
-0.236	-17.2	72.9	71.4	-3.25	-1278.0	393.0
-0.349	-26.9	75.6	74.1			
-0.479	-38.6	80.7	79.0*			
-0.585	-52.6	89.9	84.8†			
-0.591	-53.5	90.5	84.0‡			
-0.591	-53.8	91.0				
					Calculated	
				-1.347	-232.3	172.8

* Part due to second term of (7.11) 14 per cent. of whole.

† " " " 33 " "

‡ " " " 35 " "

In spite of this uncertainty there seems to be some evidence in the figures of column 4, Table IX., to show that the mathematical approximation on which (6.03) is based is getting appreciably inaccurate when d/R_1 is as large as $\frac{1}{3}$, for the numbers in column 3 are systematically greater than those in column 4 from $\mu = +0.5$ to $\mu = -0.3$.

In working out the calculated values of Ω_1/ν for negative values of μ by the formula 7.11, Part I., it is assumed that the formula ceases to be applicable when the "correction" term is more than 20 per cent. of the main term. In Table II. it will be seen that when the correction is 33 per cent., the value of Ω_1/ν is too low.

The calculated values of Ω_1/ν and Ω_2/ν for $\mu = -1.5$ in the case where $R_1 = 3.80$, and for $\mu = -1.347$ in the case where $R_1 = 3.55$ are given at the end of Tables X.* and XI.†

* See Part I. (7.13).

† See Part I. (7.14).

In order to give an idea of the uniformity of the experimental results and the accuracy of the theoretical predictions, two diagrams, figs. 17 and 18, have been prepared. In these diagrams, which may be called stability diagrams, the abscissæ represent Ω_2/ν

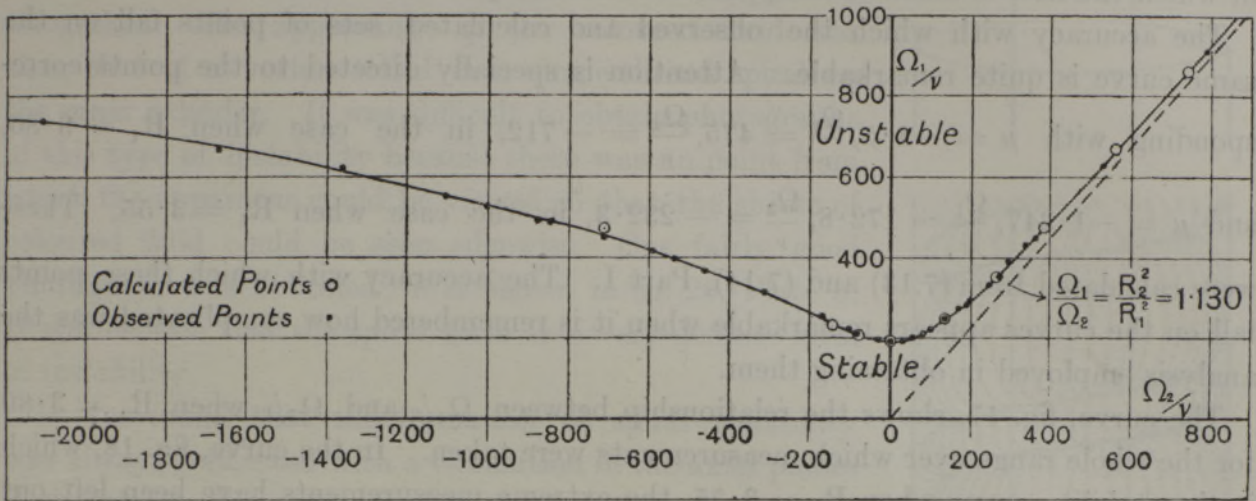


Fig. 17. Comparison between observed and calculated speeds at which instability first appears; case when $R_1 = 3.80$ cm., $R_2 = 4.035$ cm.

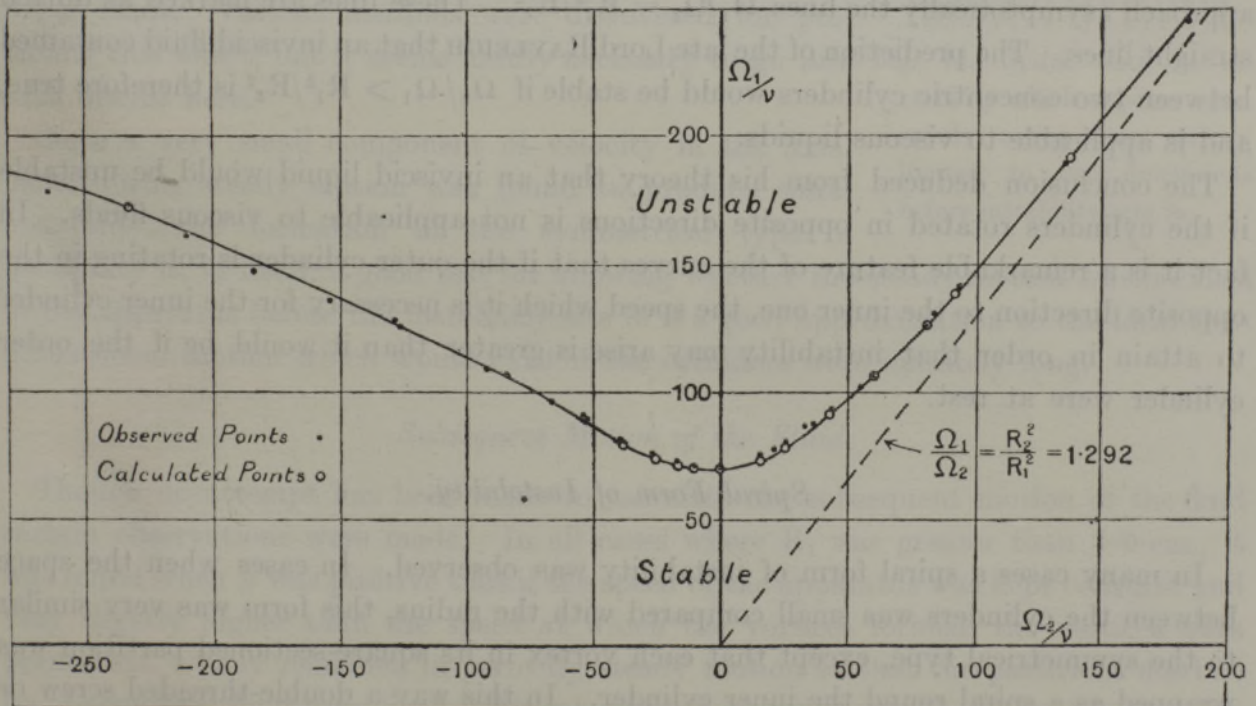


Fig. 18. Comparison between observed and calculated speeds at which instability first appears; case when $R_1 = 3.55$ cm., $R_2 = 4.035$ cm.

while the ordinates are Ω_1/ν . Every point in the diagram therefore represents a possible state of motion of the cylinders. The speeds at which instability sets in as the speed

of rotation is slowly increased are represented by points on a curve. The observed points are shown as dots while the calculated ones are shown as circles centred at the points to which they refer. All points above the curve represent states of the apparatus in which the flow is unstable while those below it represent stable states.

The accuracy with which the observed and calculated sets of points fall on the same curve is quite remarkable. Attention is specially directed to the points corresponding with $\mu = -1.5$, $\frac{\Omega_1}{\nu} = 475$, $\frac{\Omega_2}{\nu} = -712$, in the case when $R_1 = 3.80$, and $\mu = -1.347$, $\frac{\Omega_1}{\nu} = 172.8$, $\frac{\Omega_2}{\nu} = -232.3$, in the case when $R_1 = 3.55$. These were calculated from (7.13) and (7.14), Part I. The accuracy with which these points fall on the curves appears remarkable when it is remembered how complicated was the analysis employed in obtaining them.

The curve, fig. 17, shows the relationship between Ω_1/ν and Ω_2/ν when $R_1 = 3.80$ for the whole range over which measurements were taken. In the curve, fig. 18, which is the stability curve when $R_1 = 3.55$, the extreme measurements have been left out in order that the curve might be drawn on a scale large enough to give an idea of the accuracy of the results.

A noticeable feature of the results is the way in which the curves, figs. 17 and 18, approach asymptotically the lines $\Omega_1/\Omega_2 = R_2^2/R_1^2$. These lines are marked as dotted straight lines. The prediction of the late Lord RAYLEIGH that an inviscid fluid contained between two concentric cylinders would be stable if $\Omega_2/\Omega_1 > R_1^2/R_2^2$ is therefore true, and is applicable to viscous liquids.

The conclusion deduced from his theory that an inviscid liquid would be unstable if the cylinders rotated in opposite directions is not applicable to viscous fluids. In fact it is a remarkable feature of the curves that if the outer cylinder is rotating in the opposite direction to the inner one, the speed which it is necessary for the inner cylinder to attain in order that instability may arise is greater than it would be if the outer cylinder were at rest.

Spiral Form of Instability.

In many cases a spiral form of instability was observed. In cases when the space between the cylinders was small compared with the radius, this form was very similar to the symmetrical type, except that each vortex in its square-sectioned partition was wrapped as a spiral round the inner cylinder. In this way a double-threaded screw or spiral was formed, the two "threads" being vortices in the cross-sections of which the fluid rotated in opposite directions. It was noticed, however, that one of the vortices was usually wider than the other. The larger one was always the one for which the component of vorticity in the direction of the axis was the same as that of the steady motion. For instance, in the case when the outer cylinder was at rest the appearance

of the spiral would be that shown in fig. 19. The direction of rotation in the cross-sections of the spiral vortices in an axial plane is shown by means of curved arrows.

In the case where μ was < -1 the two vortices become so different in size that one of them almost disappeared altogether. The appearance of the coloured fluid was then that of a vortex rolled in a single-thread spiral on the inner cylinder. It was difficult to obtain photographs of this type of instability because there was no point from which the apparatus could be viewed so that the sheets of coloured fluid could be seen edgewise. One fairly good photograph was obtained; it is shown in fig. 20, Plate 5. It will be seen that the spiral form is a very definite form of instability.

It was found that the formation of spiral instability was always connected with a circulation in the axial planes during the steady motion before the instability appeared. In order therefore to avoid the formation of spiral instability it was necessary to avoid such a circulation in the part of the apparatus where the observations were being made. Various methods were discovered for producing this effect, but it seems hardly necessary to go into such details here.

Since a very small component of velocity in the axial plane during steady motion was found to produce spiral instability, the formation of the symmetrical type of instability is, in itself, a good test for knowing whether the steady motion which exists in the apparatus before the instability sets in is a good approximation to the ideal two-dimensional motion which would exist if the cylinders were infinitely long.

Subsequent Motion of the Fluid.

Though no attempt has been made to calculate the subsequent motion of the fluid certain observations were made. In all cases where R_1 was greater than 3.0 cm., it was found when μ was positive that if the speed of the apparatus was kept constant and very slightly higher than the speed at which the vortices formed, the vortices were permanent. They remained in perfectly steady motion so that the partitions marked by the coloured fluid were fixed. The photograph shown in fig. 11, Plate 4, is one of a steady motion which had been going for eight minutes when the photograph was taken. I do not remember to have heard of any other case in which two different steady motions are possible with the same boundary conditions. In this case evidently one of them, the two-dimensional one, is unstable; while the symmetrical three-dimensional one is stable.

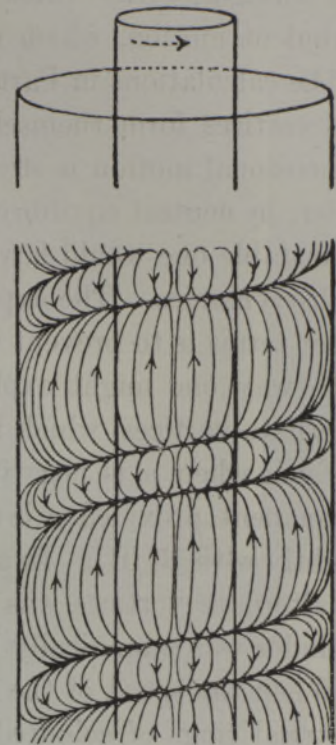


Fig. 19. Spiral form of instability which appears when steady motion is not strictly limited to two dimensions before instability sets in.

A moderate increase in the speed of the apparatus merely increased the vigour of the circulation in the vortices without altering appreciably their spacing or position, but a large increase caused the symmetrical motion to break down into some kind of turbulent motion, which it was impossible to follow by eye.

The calculations in Part I indicate that at the exact speed at which instability begins the vortices form themselves infinitely slowly. In other words the calculated three-dimensional motion is steady, to the first order of small quantities, and is, to the first order, in neutral equilibrium. To determine whether it is really steady or whether it is unstable one would have to go to the second order, a matter of extreme difficulty in hydrodynamics. The experiments described above indicate that the effect of the second order terms is to prevent the vortices from increasing indefinitely in activity. In some such way one might explain the formation of the true steady motion, consisting of alternate vortices, which is observed in the case when μ is positive.

Even when μ is negative the vortices formed when instability occurs appear to be permanent, provided μ is numerically less than a certain number which appears to vary slightly with R_1/R_2 . In all the cases when $R_1 > 3.55$ cm. it was found that the motion in alternate vortices was stable provided $-\mu < 1$, *i.e.*, when the speed of the outer cylinder was numerically less than that of the inner cylinder.

When the speed of the outer cylinder increased above this value, however, the symmetrical rings of coloured fluid which invariably appeared in the first instance if the experiment was carefully performed, were found to break up shortly afterwards. In order to find out if possible how the fluid moves during the breakdown of the first symmetrical motion a careful examination was made into the nature of the flow when μ was nearly equal to -1 . With a value of μ very slightly greater than this it was found that the breakdown occurred sufficiently slowly to enable the process to be observed by eye. Unfortunately attempts to photograph it failed, but it was sufficiently definite to be described.

Shortly after the symmetrical vortex system had formed itself, it was seen that every alternate vortex began to expand on one side and to contract on the opposite side of the cylinder. On the other hand the intermediate vortices began to expand, to fill the spaces from which the first set had contracted and to contract in the parts where the first set had expanded. The effect is represented in sketch, fig. 21.

As seen in side elevation the effect was curious; it looked as though each vortex was pulsating so that its cross-section varied periodically, though with an oscillation of increasing amplitude. After a time it became impossible to follow the motion, owing partly, no doubt, to the fact that the system adopted for marking the liquid was not really suitable for observing any but symmetrical motions.

When experiments were tried with slightly greater values of $-\mu$ it was found that the breakdown occurred in a very similar manner, but that in this case each vortex seemed to expand in several points, equally spaced, round the cylinder. The appearance of the colouring matter was then similar to that shown in the sketch, fig. 22. The

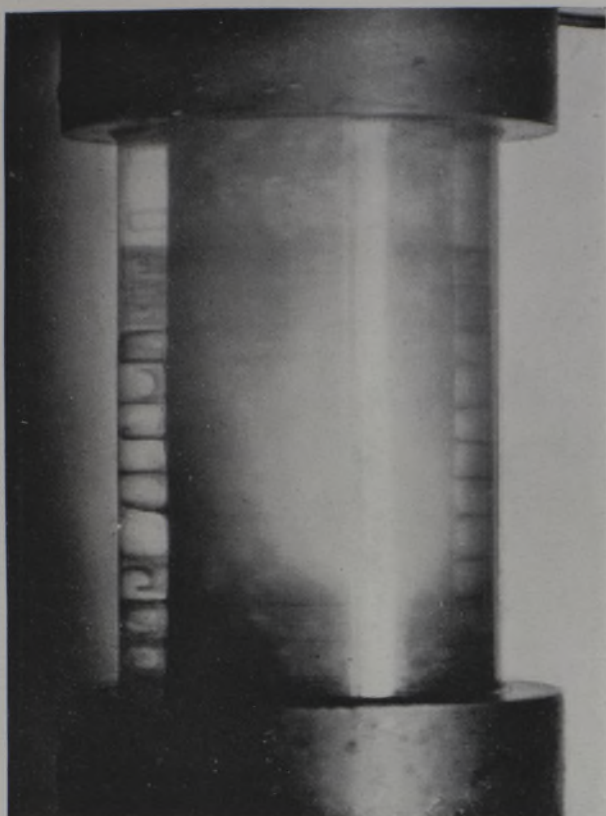


Fig. 9.

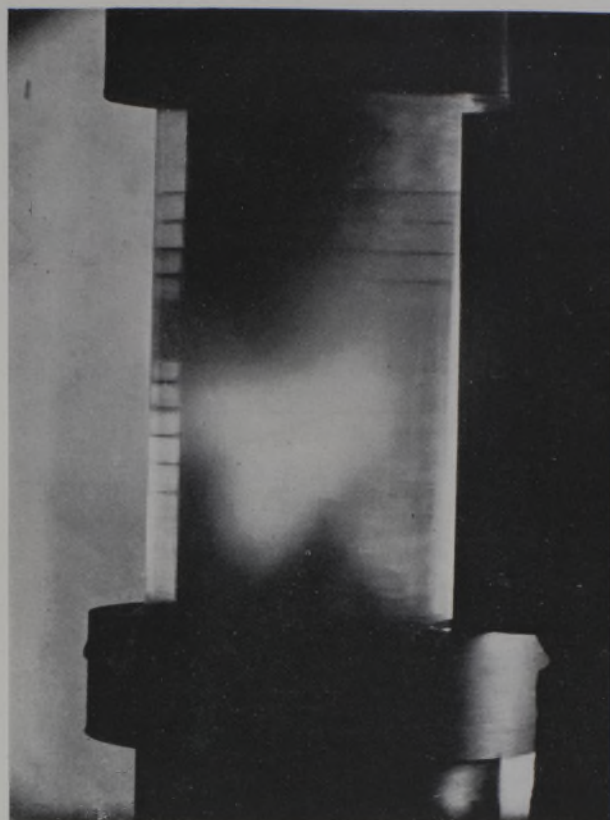


Fig. 10.

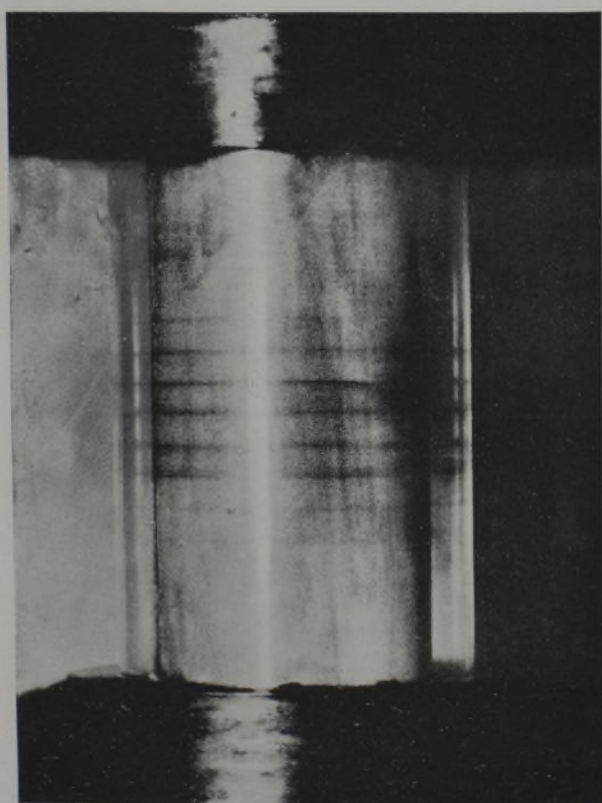


Fig. 11.

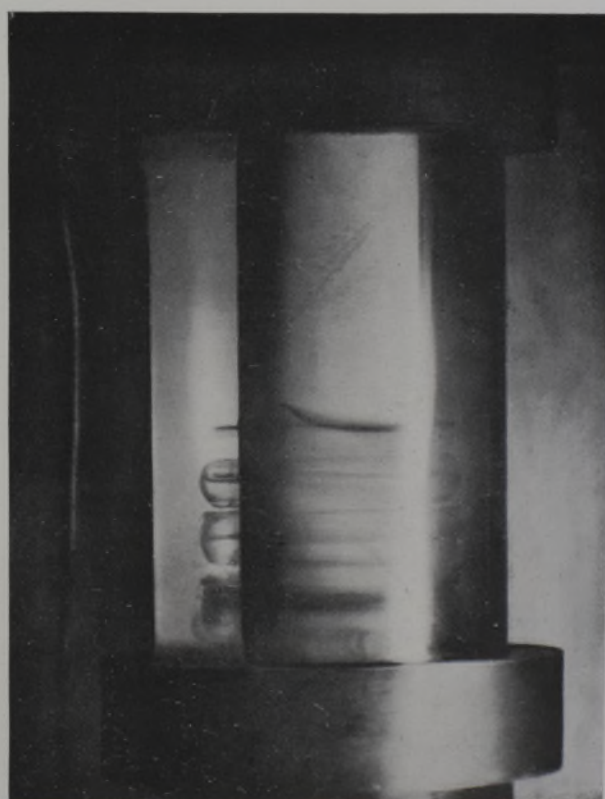


Fig. 13.

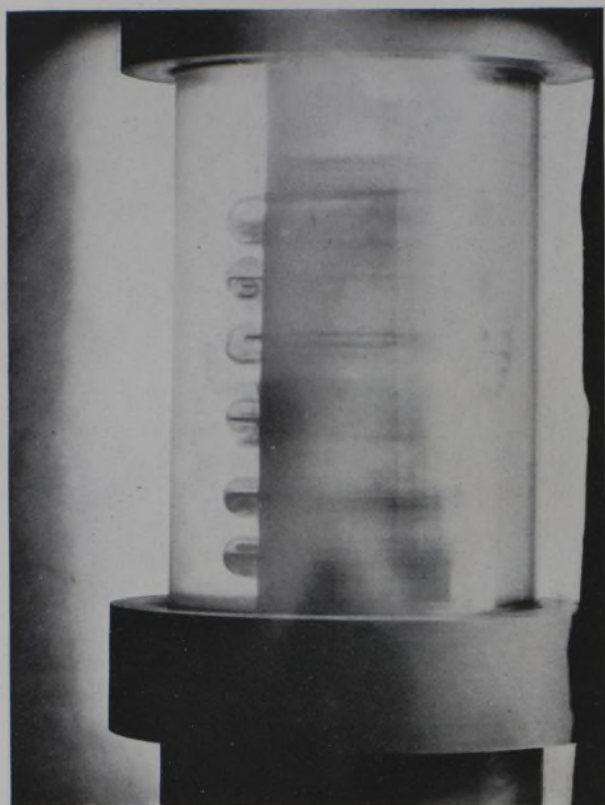


Fig. 14.

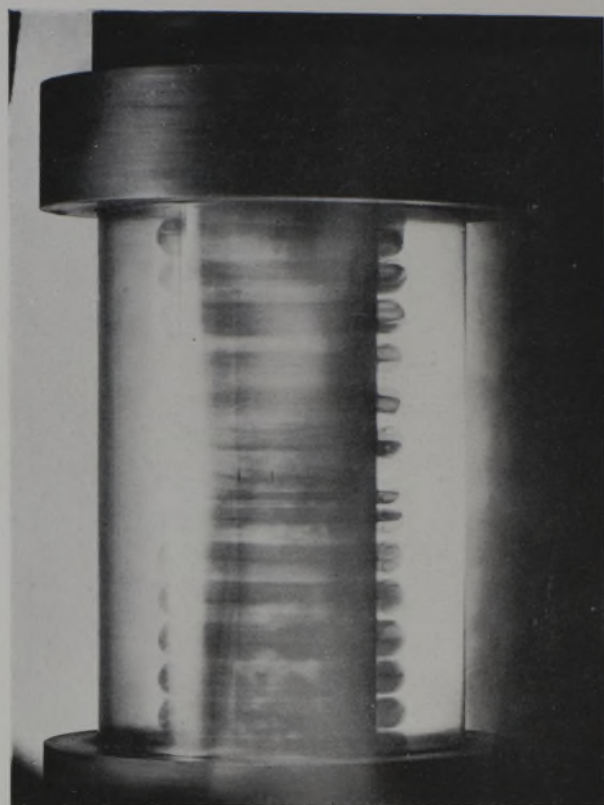


Fig. 15.

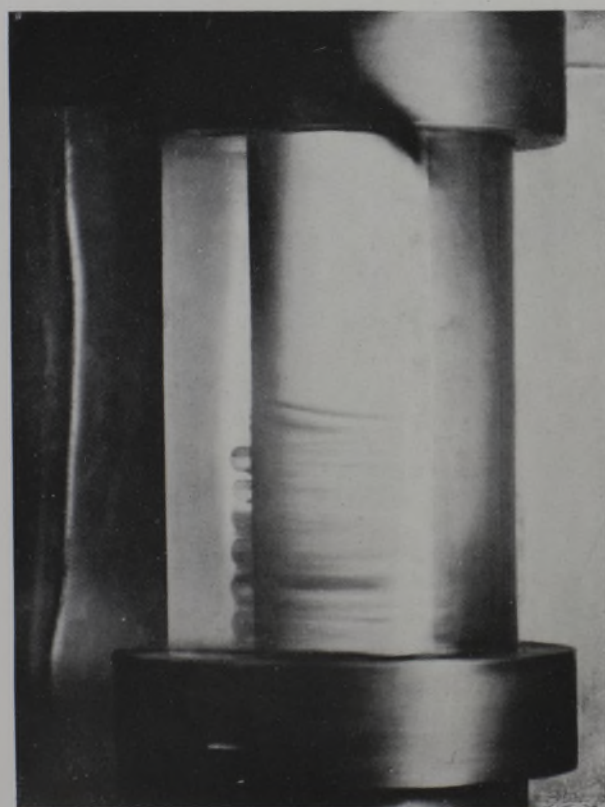


Fig. 16.

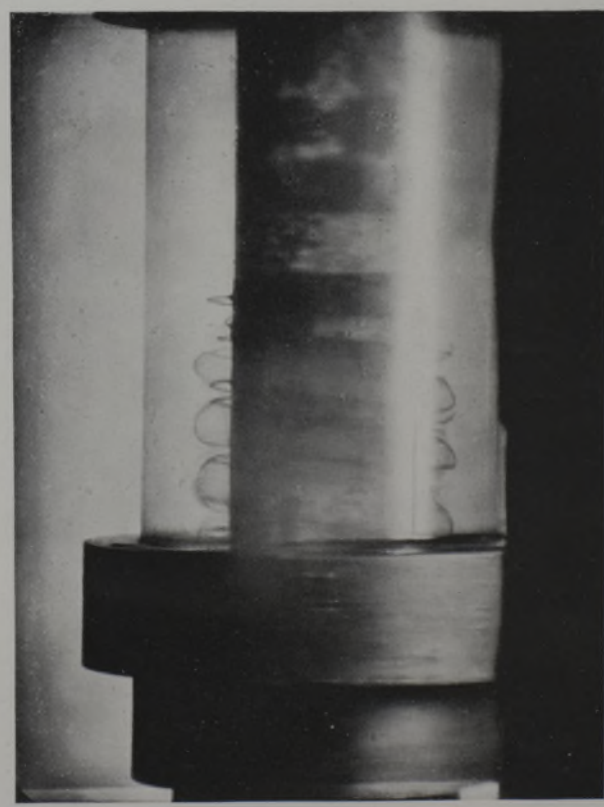


Fig. 20.

general impression gained by observing the phenomenon was that each vortex grew into the shape of a regular polygon, that these polygons were threaded on the inner

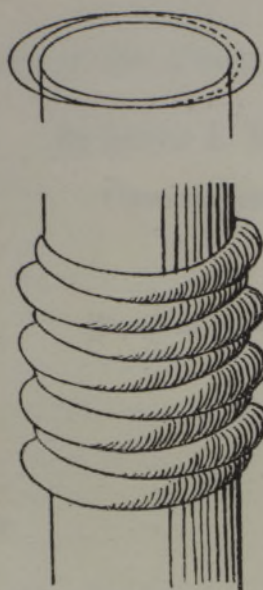


Fig. 21. Sketch illustrating appearance of vortices when they begin to break up; case when $\mu = -1$ approximately.

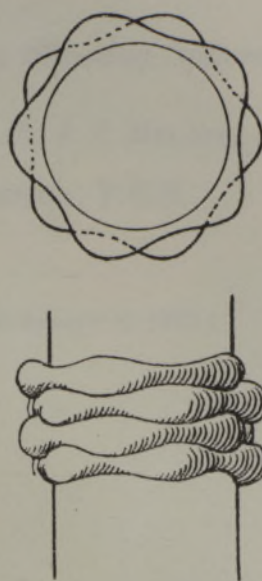


Fig. 22. Appearance of vortices when they begin to break up immediately after their formation: case when μ is less than -1 .

cylinder and rotated in the same direction, and that the corners of each polygon were placed over the sides of the one below.

DESCRIPTION OF PLATES 4 AND 5.

Fig. 9. Vortices when $R_1 = 2.93$ cm., $R_2 = 4.035$ cm., μ positive.

Fig. 10. Vortices when $R_1 = 3.25$ cm., $R_2 = 4.035$ cm., μ positive.

Fig. 11. Vortices when $\mu = 0$.

Figs. 13 and 14. Vortices when $R_1 = 2.0$ cm., $R_2 = 4.035$ cm., $\mu = -1.05$ approximately.

Fig. 15. Vortices when $R_1 = 2.0$ cm., $R_2 = 4.035$ cm., $\mu = -2.0$ approximately.

Fig. 16. Vortices when $R_1 = 2.0$ cm., $R_2 = 4.035$ cm., $\mu = -2.3$ approximately.

Fig. 20. Spiral form of instability.